Structural modelling of the Resistin family proteins and their cognate antibodies

By

Naireeta Biswas

A thesis submitted to the Johns Hopkins University in conformity with the requirements of the degree of Master of Science and Engineering.

Baltimore, Maryland

ABSTRACT

Pulmonary Hypertension (PH) is associated with the increase in blood pressure in the lung vasculature leading to fatigue, dizziness, chest pain and ultimately death. The general prognosis is survival of 2-3 years and then death caused by right ventricular failure. Research is focused on developing therapeutic methods to cure this disease.

Recent studies showed that the Resistin and Resistin-like molecule (RELM) family of proteins (adipocyte-specific hormone) are involved in the vascular remodeling and cardiac dysfunction seen in animal and human pulmonary arterial hypertension (PH). These results suggested human-resistin (hresistin) and human-RELMβ (hRELMβ) are important for the etiology of human PH and are potential biomarkers and therapeutic targets for this disease. This led to development of a series of human antibodies that target distinct and common epitopes of hresistin and hRELMβ by the members of Dr. Roger Johns' research group. My goal is to create 3-d models of these antibodies in complex with hresistin + hRELMβ to gain insight into their functions.

Using homology modelling techniques such as SWISS-MODEL and MODELLER, I predicted the three-dimensional structures of hresistin and hRELMβ, using the crystallographic structures of mouse-resistin and mouse-RELMβ. Using RosettaAntibody protocol, I modelled the three-dimensional structures of a series of 32 human antibody sequences designed specifically to target hresistin and hRELMβ. These models confirmed the antibody's stability and suitability. The predicted structures of these 32 antibodies validated that they were designed conforming to the standard structural parameters of naturally occurring human antibodies. Experimental studies showed that hresistin and hRELMβ exist in multimer states but that the monomer form is the most functional. Therefore, using the SnugDock protocol in Rosetta, I docked each of the antibodies to hresistin and hRELMβ monomeric forms. From the docking results, I identified the most-likely antibody-antigen docked state using model energies. From the docked structure of each antibody-antigen complex, I extracted the epitope regions of hresistin and hRELMβ. The models suggest that the lead antibody, antibody AntiRes13 binds strongly to the head

region of hresistin and strongly to the tail region of hRELMβ. The docking results of antibody AntiRes-13 also validated its corresponding antigen binding experiments. Out of the set of 32 antibodies, antibody AntiRes-2, 3, 9, 11 and 41 also showed positive binding affinities to the antigens. In the models, AntiRes-2 binds hresistin at the head and hRELMβ at the head. Antibody AntiRes-3 binds the tail region of hresistin and head region of hRELMβ. Antibodies AntiRes-9 and AntiRes-11 bind to the head regions of both hresistin and hRELMβ whereas AntiRes-41 prefers to bind the tail region of both antigens. This project gives insight into design for potential therapeutic applications for curing PH.

Advisor: Dr. Jeffrey J. Gray

ACKNOWLEDGEMENT

I would like to extend my gratitude to Prof. Jeffrey J. Gray for accepting me and allowing me to work within his research group at Johns Hopkins University. I would like to thank prof. Roger A. Johns for the collaboration in such an interesting research project. The completion of this project was solely due to insights provided to me by Prof. Gray and Prof. Johns.

I would also like to extend my appreciation to all the members of the GrayLab group especially Dr. Nick Marze and Jeliazko Jeliazkov who have helped me immensely in understanding the Rosetta software and its workings. I would also like to thank Chunling Fan for all the information and insight on the experimental work. The knowledge gained helped me immensely in my thesis. I would also like to thank Joseph Lubin for the friendship and support.

Lastly, I would like to thank my parents for being my support system throughout this whole process.

Table of Contents

LIST OF FIGURES

Figure.4.20: Comparison of the docking results of AntiRes-13 with hresistin (blue) to the docking results of AntiRes-13 with hRELM (orange). The results showed that there is no consensus in the binding locations.

LIST OF TABLES

CHAPTER I

INTRODUCTION

I. Pulmonary Hypertension

Pulmonary Hypertension (PH) is a severe disease of the lung vasculature leading to right heart failure and death. It is defined as an increase in blood pressure in the pulmonary artery, pulmonary vein or pulmonary capillaries which leads to shortness of breath, dizziness, fainting and other symptoms ultimately causing death[1-8]. There is no currently cure for this disease, and most current therapies provide only limited relief. According to latest classification there are six different types of pulmonary hypertension, all leading to a common endpoint[4].

Pulmonary arterial hypertension is caused due to the narrowing of the blood vessels connected to or within the lungs[2,4]. This makes it difficult for the heart to pump blood to the lungs. Over time the blood vessels develop fibrosis which further increases the blood pressure. The increased workload of the heart causes hypertrophy of the right ventricle ultimately causing right heart failure. As the blood flowing through the lungs decreases, the left side of the heart receives less blood. This blood may also carry less oxygen than normal. Therefore, it becomes harder and harder for the left side of the heart to pump to supply sufficient oxygen to the rest of the body. The general prognosis is survival for 2-3 years from the time of diagnosis and ultimately leading to death[7,8].

II. Resistin and RELM proteins

Resistin initially was identified in rodents as adipose-tissue-specific-secretory-factor (ADSF) which was associated with diabetes[19-22]. It was observed that resistin played a role in glucose metabolism and insulin resistance. Circulating levels of resistin in the blood of mice were down regulated by anti-diabetic drugs and experimental modification led to changes in the blood glucose and insulin function[19-22]. During the characterization, of human resistin it was observed that it expresses in macrophages rather than in the adipose tissues. Also, the levels of the circulating resistin are associated with inflammation[21,22].

During initial characterization of resistin, additional resistin-like genes were identified[21,22]. Currently apart from resistin, three other members were observed in mice which are RELMα, RELMβ and RELMγ. One more member was observed in humans which is RELMβ[19-20].

Proteins in the resistin family have a unique structure with no known homology to any other proteins. Both human and rodent variants contain between 105 and 117 amino acids with notable interspecies (33%-59%) and intra-species (21-51%) homology[19-22]. The common feature of these proteins is the presence of five disulfide bonds formed by cysteine signature motif ($CX_{11}CX_8CXCX_3CX_{10}CXCXCX_9CC$) in the c-terminal part of the protein that forms a monomer consisting of a globular head and a helical tail[19].

During the process of investigating the function of human resistin using recombinant protein expressed and produced from HEK293 cells, it was found

that hresistin and hRELMβ exist as three species: monomer of a low-molecular-weight (LMW) at approx. 13kDa, a medium-molecular weight (MMW) dimer of ~ 26kDa formed by a disulphide bond between the terminal tail of two monomers, and a high-molecular-weight hexamer at ~ 50kDa made up of three dimers twisted together[14-16]. The formation of intermolecular disulphide bonds between cysteine 22 in human resistin is essential for resistin multimerization and secretion. Different molecular isomers of human resistin may exhibit differences in bioactivity, like human adiponectin, another family of proteins with similar structure to resistin.

III. Association of the protein with PH

The resistin-like molecule (RELM) family of proteins comprises pleiotropic cytokines critically involved in the vascular remodeling and cardiac dysfunction seen in animal and human PH. Dr. Roger Johns laboratory discovered the RELM family of proteins in PH lung as a "hypoxia-induced mitogenic factor (HIMF)"[9-14]. They demonstrated that these proteins have pro-inflammatory, proliferative, vasoconstrictive, and chemokine actions and the ability to induce the vascular remodeling and hemodynamic changes of PH in rodent models (gain of function)[9-14]. Inhibition of this pathway by adeno-associated virus (AAV) shRNA against HIMF or knockout of HIMF prevents the development of hypoxia-induced PH (loss of function)[15-17]. Their subsequent work further validated human resistin (hresistin) and human RELMβ (hRELMβ) as therapeutic targets for human PH. They found that hresistin and hRELMβ were upregulated in the lung hypertrophic vasculature and other regions of patients suffering from pulmonary hypertension. The

RELM proteins induce cardiac hypertrophy, cardiac fibrosis, and dysfunctional sarcomere shortening[18-22]. They identified specific polymorphisms in hresistin and hRELMβ associated with development of PH within patient population, some of which correlate with serum resistin level and with biochemical and clinical markers of heart failure. These results suggested that hresistin and hRELMβ are mechanistically important to the etiology of human PH and may serve as potential biomarkers and therapeutic targets for this disease.

IV. Goals of my thesis

My thesis work is a collaboration with members of Dr. Roger John's laboratory from Johns Hopkins School of Medicine who provided the experimental support necessary to compare with my computational models. The main goals of my thesis are as follows:

i. **Predict the three-dimensional structures of hresistin and hRELMβ:** As there are no crystallographic structures of the proteins, it was necessary to understand the structural significance of these proteins and the role their various multimer form plays.

ii. **Model structures of human antibodies:** Using a human S_CF_V library, 32 human IgG1 antibody sequences were selected specifically to target hresistin and hRELMβ. I modelled all the 32 antibodies sequences using RosettaAntibody. The models of these antibodies were usedto estimate their binding affinities and epitopes.

iii. **Docking human antibodies with hresistin and hRELMβ:** Using SnugDock, I docked the each of the antibodies with the

target antigens. I predicted the best docked state of each of the antibody-antigen complexs which I further analyzed to determine the potential epitope regions of the target antigens.

The results from my work are a step towards the goal of building a successful therapeutic model for curing Pulmonary Hypertension. My project gives an in-depth insight regarding the key molecules associated with PH.

CHAPTER II

HOMOLOGY MODELLING OF RESISTIN PROTEINS

I. Overview

To generate the homology models of hresistin and hRELMβ, we first obtained the amino acid sequences of all the members of the resistin-like-molecule family. Crystal structures of mresistin (PDB code 1RFX) and mRELMβ (PDB code 1RH7) were available[61]. I obtained a complete sequence alignment of all the six members of the family. I performed a BLAST searcg using the PDB structures of mresistin and mRELMβ as templates respectively [23-31]. The results from BLAST revealed the sequence identity of the resistin-like proteins with respect to each of the templates. This allowed me to construct a phylogenetic tree. The phylogenetic tree determines the optional PDB structure to use as template to build the homology models of the rest of the proteins in the family. The homology models were generated using the SWISS-MODEL[32-35] and MODELLER[36-39] programs. SWISS-MODEL and MODELLER are software packages used for homology and comparative modelling of protein three-dimensional structure. The first generation of models obtained from the programs were optimized using *Rosetta* Relax protocol to produce our final models[44+46]. The flowchart (Figure.2.1) summarises the methodology.

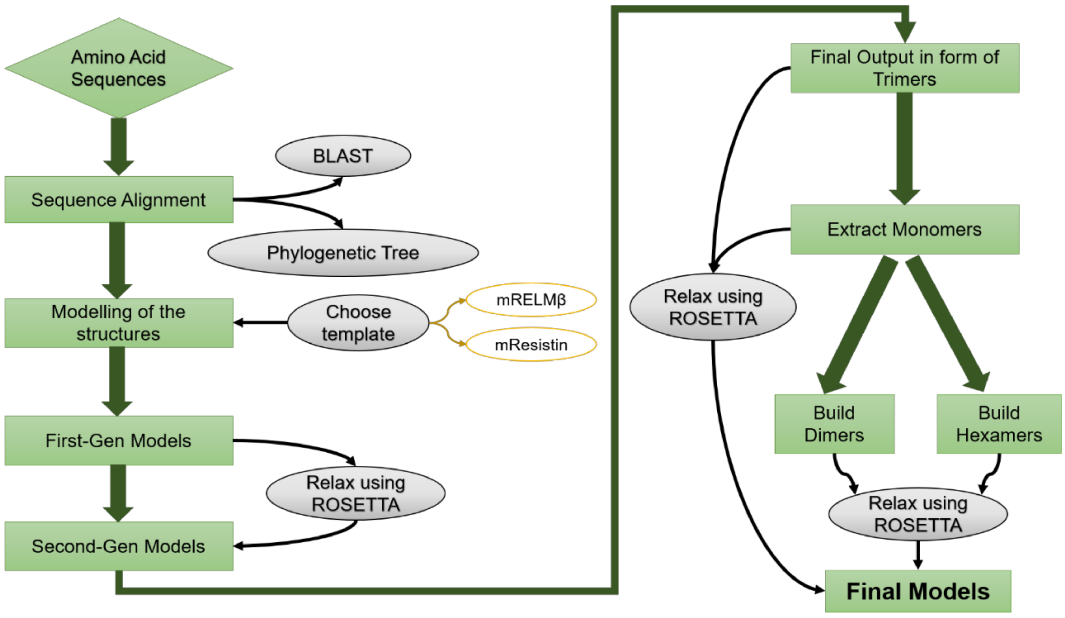

Figure.2.1:Flowchart of the overview of the homology model process.

II. Comparing homology with existing PDB structures

From literature study, I know that mresistin and mRELMβ already exist as crystal structures. Before using these structures as templates for building the models of its human relatives, we compared the two structures to determine the sequence and structural similarity. Comparison of the existing crystal structures with the rest of members of the proteins was necessary. This comparison helped me to determine which crystal structure can be best used as a template to model the correct homologous structures of hresistin and hRELMβ.

Structurally, the head region consists of six β-sheets. These β-sheets are connected via stable disulfide linkages formed by the cysteine motif, thus forming a jelly-roll-topology (Figure 2.2). The tail region consists of a long helix chain of roughly twenty residues in length.

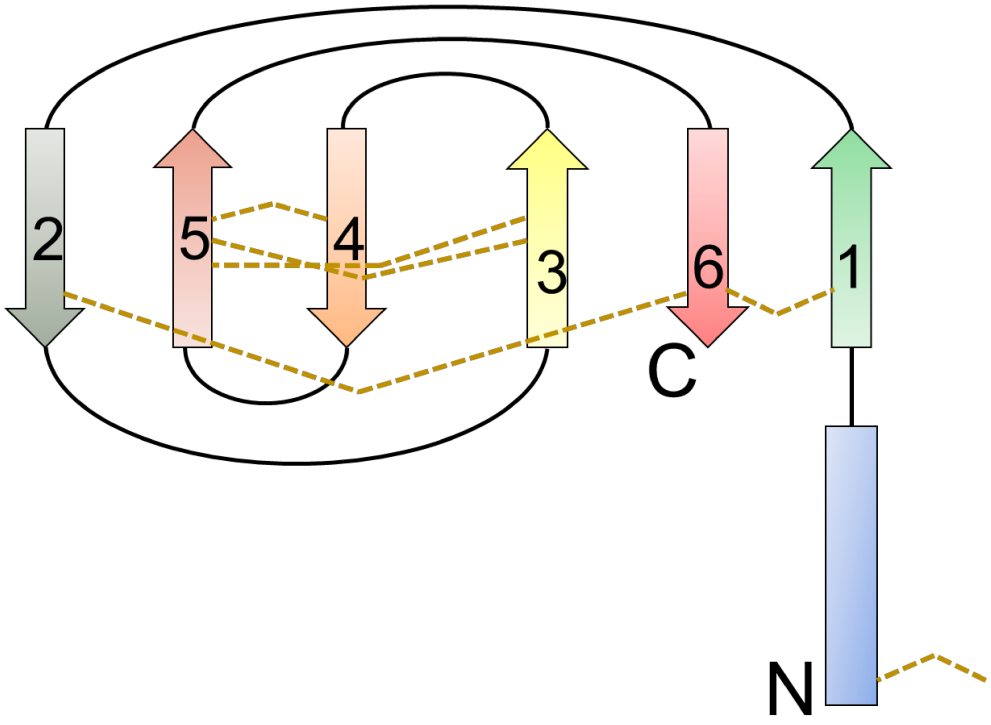

Figure.2.2: Diagrammatic representation of the resistin motif. The dashed lines represent the disulfide bonds highlighting the jelly like topology.

I performed sequence alignment using ClustalOmega[40-42]. ClustalOmega is a multiple sequence alignment tool that aligns different protein sequences and predicts the sequence similarity. From the sequence alignment(Figure2.3), I can see that the cysteine rich motif is conserved and consistent amongst all the members of the family. It also shows that amongst all the members, the homology is conserved within the head region is more conserved while the N-terminal tail region is more diverse.

```
hRELM-beta      MGPSSCLLLILIPLLQLINPGSTQCSLDSVMDKKIKDVLNSLEYSPSPISKKLSCASVKS
mRELM-beta      MKPTLCFLFILVSLLPLIVPGNAQCSFESLVDQRIKEALSRQ------EPKTISCTSVTS
mRELM-alpha     MKTTTCSLLICISLLQLMVPVNTDETIEIIVENKVKELLANPANYPSTVTKTLSCTSVKT
mRELM-gamma     MKTTTCSLLICISLLQLMVPVNTEGTLESIVEKKVKELLANRDDCPSTVTKTFSCTSITA
mResistin       ------------------SSMPLCPIDEAIDKKIKQDFNSLFPN-AIKNIGLNCWTVSS
hResistin       ---MKALCLLLLPVLGLLVSSKTLCSMEEAINERIQEVAGSLIFR-AISSIGLECQSVTS
                                    ::  :::::::              :.* ::.:

hRELM-beta      QGRPSSCPAGMAVTGCACGYGCGSWDVQLETTCHCQCSVVDWTTARCCHLT---
mRELM-beta      SGRLASCPAGMVVTGCACGYGCGSWDIRNGNTCHCQCSVMDWASARCCRMA---
mRELM-alpha     MNRWASCPAGMTATGCACGFACGSWEIQSGDTCNCLCLLVDWTTARCCQLS---
mRELM-gamma     SGRLASCPSGMTVTGCACGYGCGSWDIRDGNTCHCQCSTMDWATARCCQLA---
mResistin       RGKLASCPEGTAVLSCSCGSACGSWDIREEKVCHCQCARIDWTAARCCKLQVAS
hResistin       RGDLATCPRGFAVTGCTCGSACGSWDVRAETTCHCQCAGMDWTGARCCRVQP--
                 .  ::** * .. .*:** .****:::   .*:* *  :**: ****::
```

Figure.2.3: The sequence alignment of all the members of the Resistin family of proteins.

I next performed a BLAST analysis to determine the percentage homology amongst the different members and to determine the phylogenetic tree. The BLAST analysis determines regions of local similarity between sequences. This program can compare nucleotide or protein sequences to sequence databases and calculates the statistical significance of matches. BLAST is also used to infer functional and evolutionary relationships between sequences. It also helps identify members of gene families. The BLAST results gave me the percentage identity of each of the members of the resistin-like protein family with respective crystal structures of mresistin and mRELMβ (Table.2.1). I observed that hresistin has higher sequence identity to mresistin than to mRELMβ as it has a 58% sequence identity whereas hRELMβ is more homologous to mRELMβ with 57% sequence identity.

I also generated the phylogenetic tree which showed the similarity (Figure.2.4). The phylogenetic tree shows that mresistin and hresistin are more closely related to each other than to the RELMβ molecules. Similarly, mRELMβ is more closely related to hRELMβ. These results helped me to

choose the templates for building the homology models. For homology modelling a minimum of 50 to 60 % sequence identity is required as the results satisfied the conditions to pursue it. Based on the sequence alignment results, I observed that members of this protein family are likely to have the well conserved jelly roll like topology. Therefore, I decided to use the mresistin (PDBID 1RFX) as template to model hresistin and mRELMβ (PDBID 1RH7) to model hRELMβ.

Protein Name	%Identity to mresistin	%Identity to mRELMβ
Human Resistin (hresistin)	58	49
Human RELM-β (hRELMβ)	52	57
Mouse RELMα(mRELMα)	38	50
Mouse RELM-γ (mRELMγ)	41	63

Table.2.1: The BLAST analysis showing the percentage sequence identity of the resistin family of proteins.

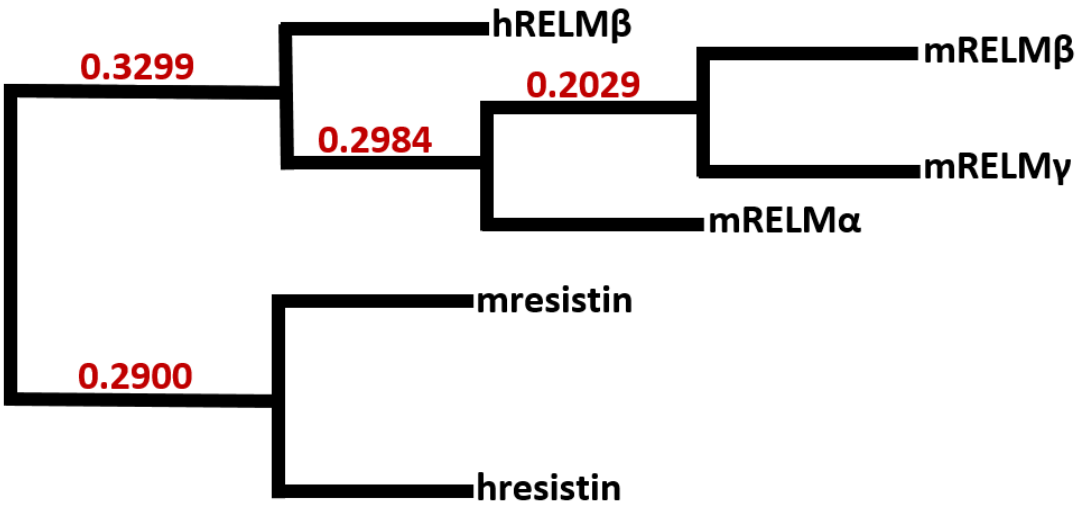

Figure.2.4: The phylogenetic tree of selected members of the Resistin family of protein.

III. Building different multimeric structures

In chapter I, resistin family proteins exist in various multimer states. Experimental results performed in Dr. Roger John's laboratory revealed these various multimer forms of the hresistin and hRELMβ. A non-reducing SDS-PAGE gel experiment was conducted by my collaborator Chunling Fan, where the C-terminal FLAG-tagged recombinant murine and human RELM proteins were overexpressed in Flp-in T-Rex 293 cells under the induction of tetracycline and purified with FLAG affinity chromatography. Purified recombinant RELMs (2-3μg/sample) mixed with non-reducing Laemmli loading buffer (no reducing reagents used) and were loaded onto Tris-HCl 4-20% gradient SDS-polyacrylamide gels (Bio-Rad). After separation, the proteins in the gel were stained by Coomassie brilliant blue after fixation (Figure.2.5 and Figure.2.6).

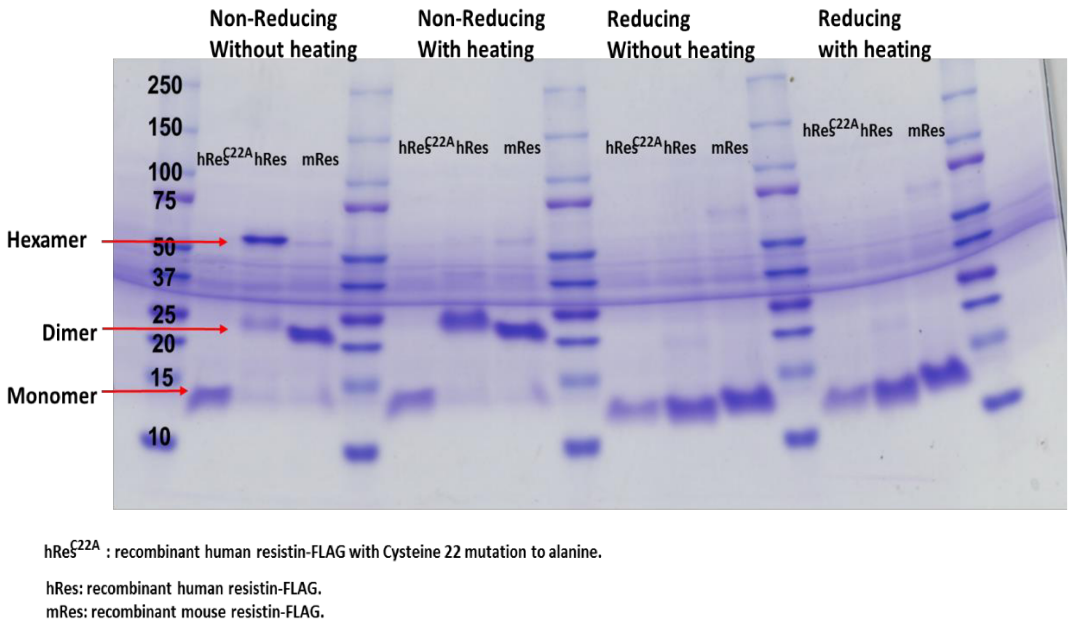

hRes^{C22A} : recombinant human resistin-FLAG with Cysteine 22 mutation to alanine.

hRes: recombinant human resistin-FLAG.
mRes: recombinant mouse resistin-FLAG.

Figure.2.5:SDS-PAGE results showing the different multimer states of hresistin and mresistin (from Chunling Fan).

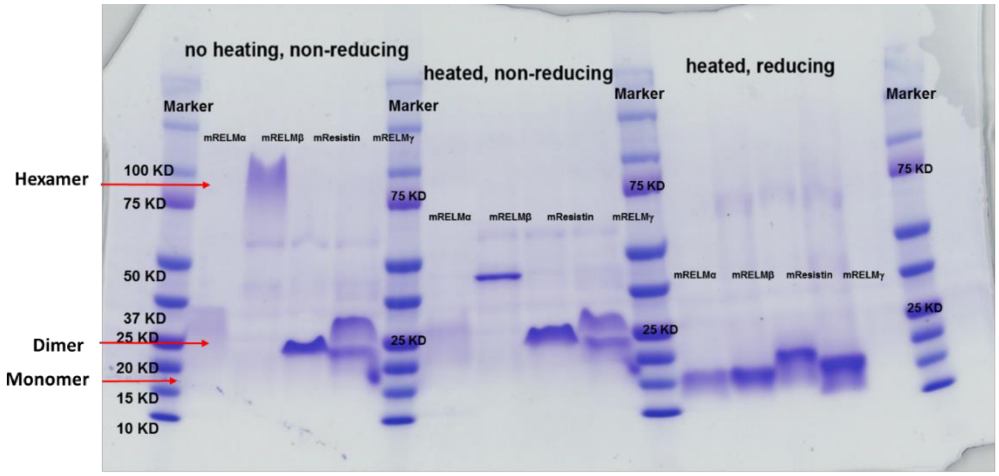

Figure.2.6:SDS-PAGE results showing the different multimer states of mRELMβ (from Chunling Fan)

From the SDS-PAGE results, I concluded that hresistin and hRELMβ exist in different multimer forms such as monomer, dimer and hexamer (Table.2.2). The hexamer state of the proteins are the native states of the proteins.

PROTEIN	HEXAMER	DIMER	MONOMER
mresistin	-	**Native State**	On **reducing** and **heating**
mRELMα	-	-	Always
mRELMβ	**Native State**	On **reducing** form Trimer	On **heating** and **reducing**
mRELMγ	-	**Native State**	On **heating** and **reducing**
hresistin	**Native State**	On **heating**	On **reducing** and **heating**
hRELMβ	**Native State**	On **reducing**	On **heating** and **reducing**

Table.2.2: The different multimeric states of the resistin family protein summarized from Chunling Fan's data

Using SWISS-MODEL and MODELLER software packages, I built the first generation of hresistin and hRELMβ structure models. I created the models generated as homo-trimers, mimicking the crystal states of the template PDB structures (Figure.2.7). The models were optimized using the Rosetta Relax protocol. The Relax protocol is used for simple all-atom refinement of structures. It is used to avoid non-ideal geometry of the protein structures.

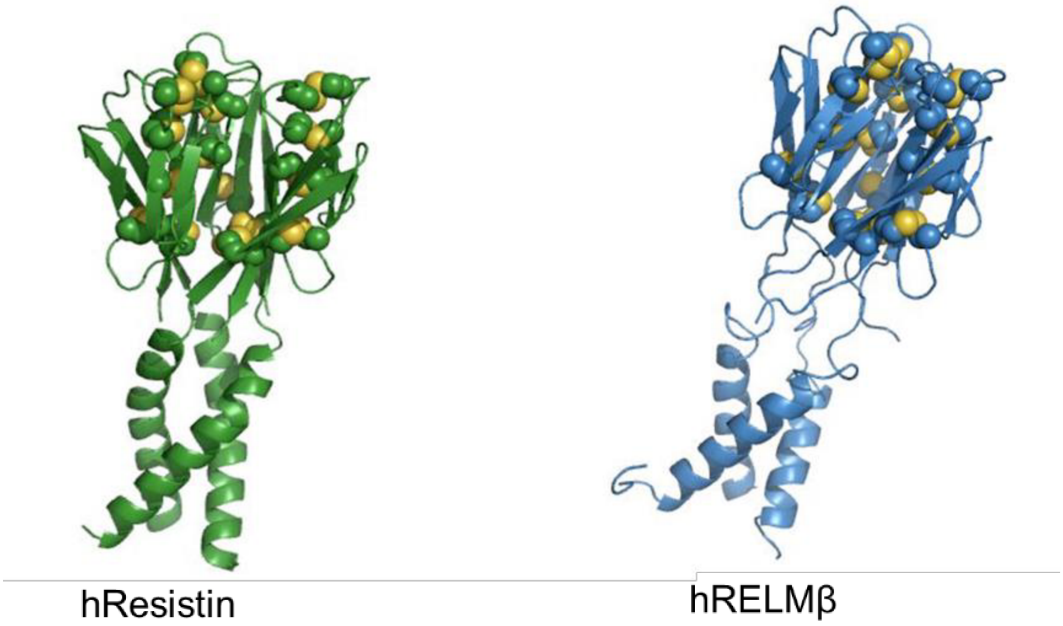

Figure.2.7: The homo-trimer state of hresistin and hRELMβ mimicking the crystal state of mresistin and mRELMβ.The disulfide bonds are highlighted with spheres.

I compared the models generated with their respective templates and I observed the structural similarity (Figure.2.8). I observed that hresistin and mresistin are structurally similar with a Cα atom root mean squared deviation of 0.70Å. The structural similarity between hRELMβ and mRELMβ is a lower with RMSD value calculated to be 0.584Å. This difference in structural similarity between hRELMβ and mRELMβ is due to the high diversity of the helical tails.

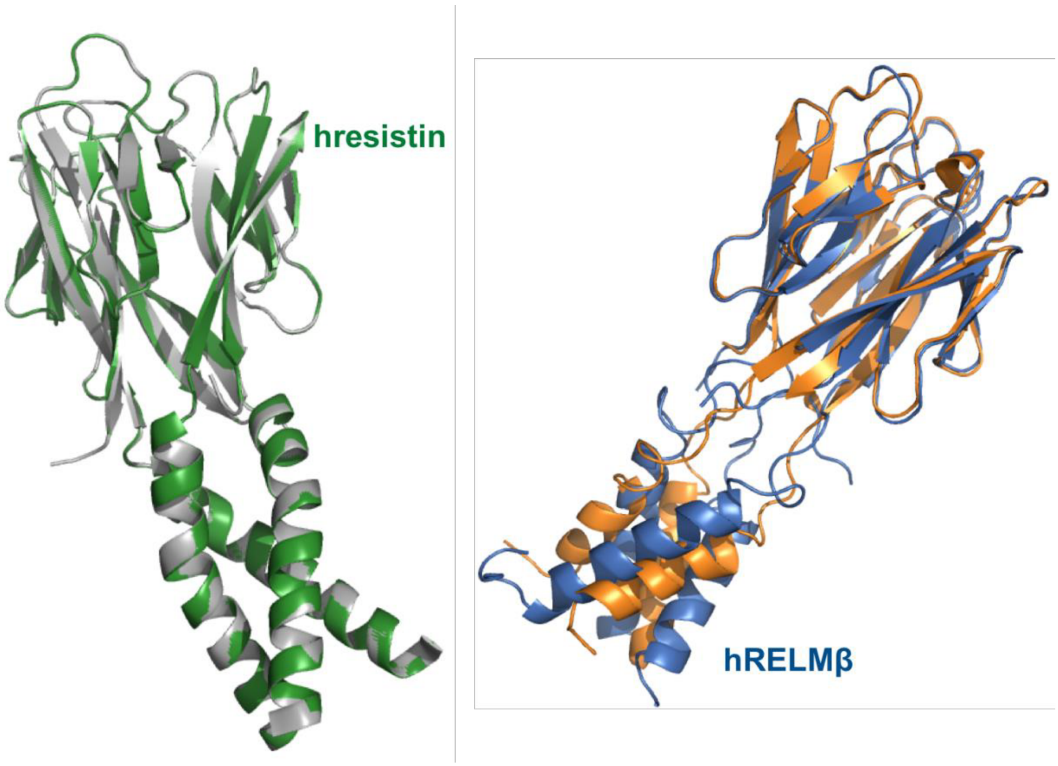

Figure.2.8: Comparison of the structural similarity of hresistin(green) with mresistin(gray) and of hRELMβ(blue) with mRELMβ(orange)

I also compared the structural similarities between the hresistin and hRELMβ. The RMS value calculated to be 2.598Å. This shows that there is structural diversity between both the proteins. The diverse feature is observed in their helical tails (Figure.2.9). The helical tail for hresistin is more defined while the tail of hRELMβ has large floppy regions. This is because of the presence of proline residues which show less helical propensity, thus breaking the helical cone formation.

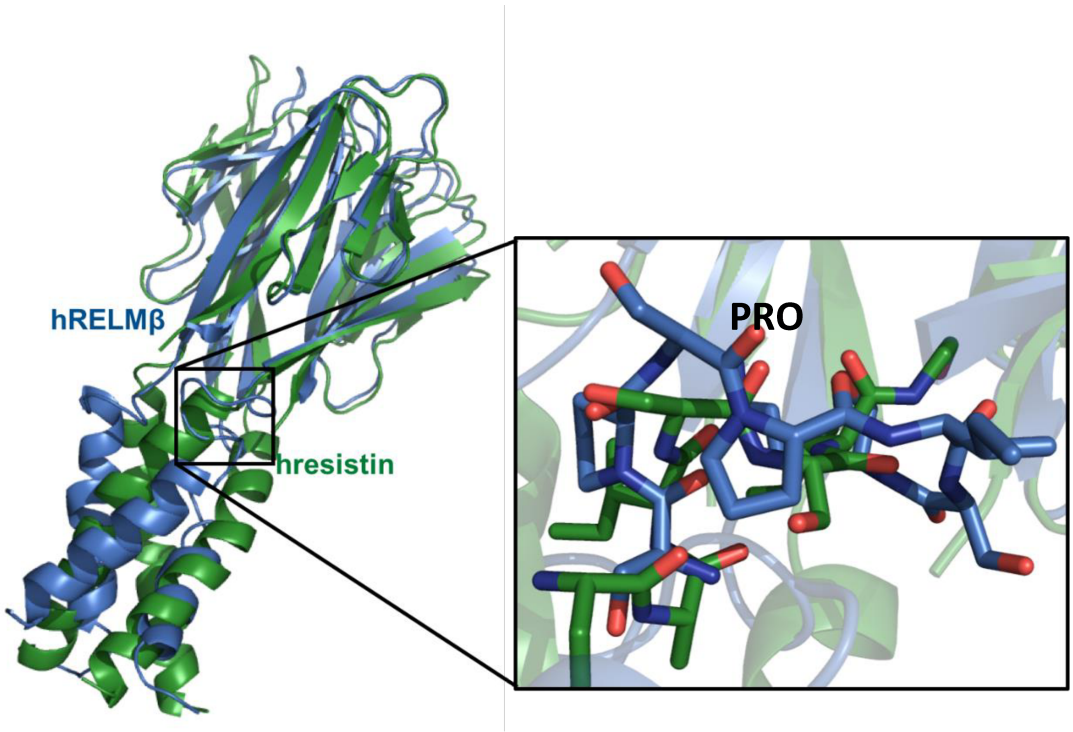

Figure.2.9: Structural comparison between hresistin and hRELMβ showing that presence of proline residue tends to break the helical chain formation

From the homo-trimer states of the hresistin and hRELMβ, I extracted the monomers. I optimized the monomer states using the Rosetta Relax protocol. This optimization finally generated the monomer models of hresistin and hRELMβ (Figure.2.10 and Figure.2.11).

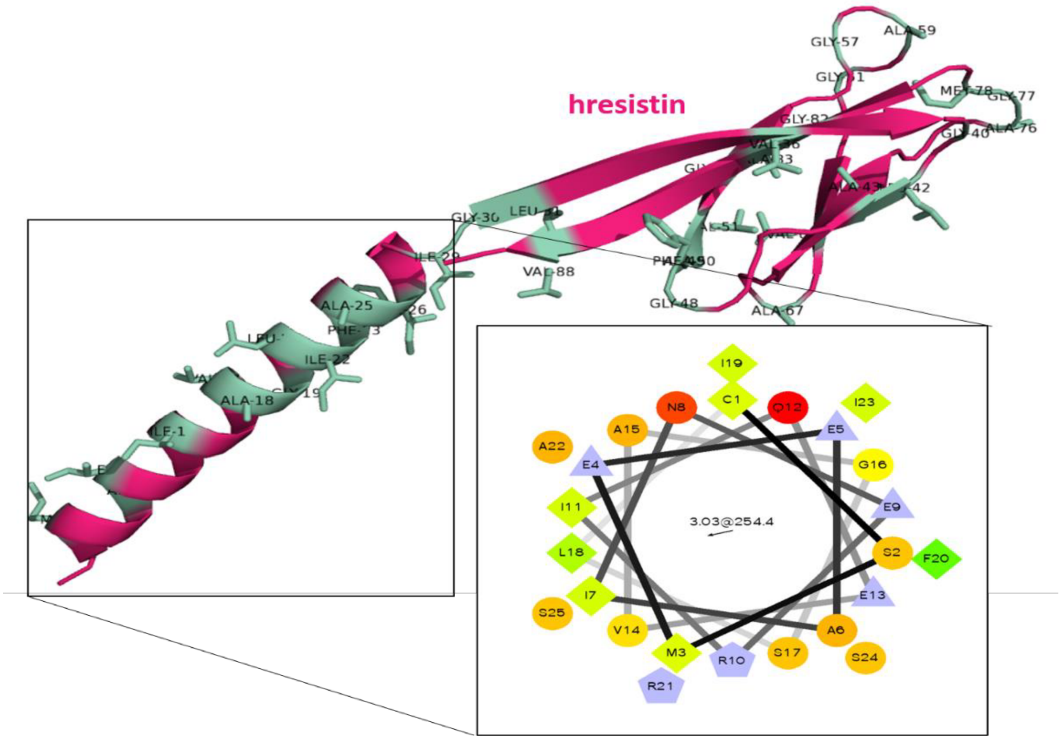

Figure.2.10: Monomer form of hresistin along with the helical wheel. The regions highlighted in pale sea green show the hydrophobic regions.

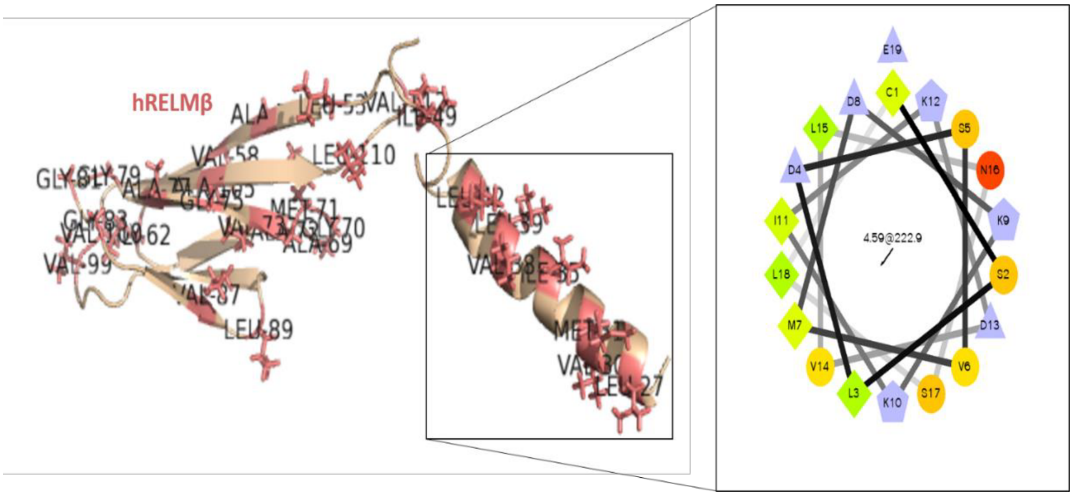

Figure.2.11: Monomer form of hRELMβ along with the helical wheel. The regions highlighted in peach show the hydrophobic regions

I also generated the helical wheel for both monomers. A helical wheel is a visual representation of the distribution of residues around the alpha helices

of the proteins. The helical wheel reveals the hydrophobic regions as diamonds, hydrophilic residues as circles, potentially negatively charged as triangles and potentially positively charged as pentagons. I observed that the helical tails of the proteins are highly hydrophobic in nature. This can influence the antibody-antigen docking positions.

The hexameric forms of the proteins is visualized as the dimer of the trimer states of the proteins. From experimental studies, it has been observed that the monomeric form of the proteins are most likely to be the functional form of the protein rather than its native hexamer state. Hence, for my further research I focused on the monomer and trimer state of the proteins. Generating a structural model and understanding the structural properties of the proteins is important for determining its binding specificities with antibodies. This aspect will be discussed further in the future chapters.

CHAPTER III

MODELLING OF THE COGNATE ANTIBODIES

I. Computational Methodology

All the antibodies that were designed by the members of the John lab, I computationally modelled them using the RosettaAntibody protocol[47-49]. This protocol predicts the three-dimensional structure of the antibody based on the sequences. This protocol focusses on modelling the F_V region of the antibody as it contains the variable region that binds antigens. The F_V region is divided into two regions -the framework and the CDR loops. The framework is highly conserved and thus accurate structures of the regions are modelled using the template structures[47-49]. The CDR loops are known to have distinct structures. Five out the six loops are modelled based on the canonical loop conformations[47-49]. These five loops based on so called canonical conformations are modelled using template structures. The sixth loop, the CDR H3 loop does not follow any canonical conformation and must be modelled *de-novo*. As the H3 loop lies between two domains (V_H and V_L) the V_H-V_L orientation is also optimized in the protocol[49,50].

The structural model of the antibody is determined from the sequences using homology modelling techniques. The RosettaAntibody protocol identifies the CDR loop regions from the amino acid sequence and renumbers them based on the Chothia numbering scheme. Based on highest sequence similarity, a template is selected for each of the structural components- framework and CDR loops. Initial V_H-V_L orientations are also set by selecting templates.

After this the CDR templates are grafted on each of the framework regions of the antibody. Then 10 initial grafted models are generated of the antibody. The CDR clusters for each of the loops are checked using the North CDR Clustering library[51-53] to make sure that the correct templates have been chosen for modelling the antibody. The grafted models are further refined. The CDR H3 loop is remodeled and the V_H-V_L orientation is recalculated to consider the remodeled H3 loop. The first grafted model is used to generate 1000 refined models. The subsequent grafted models are used as starting for 200 refined models. Thus, 2800 candidate structures are generated. The V_H-V_L orientations are checked by generating LHOC plots[49]. All the 2800 models are sorted based on Rosetta score. The lowest energy models are considered the most favorable antibody structures. The complete methodology is shown as a flowchart in Figure.3.1.

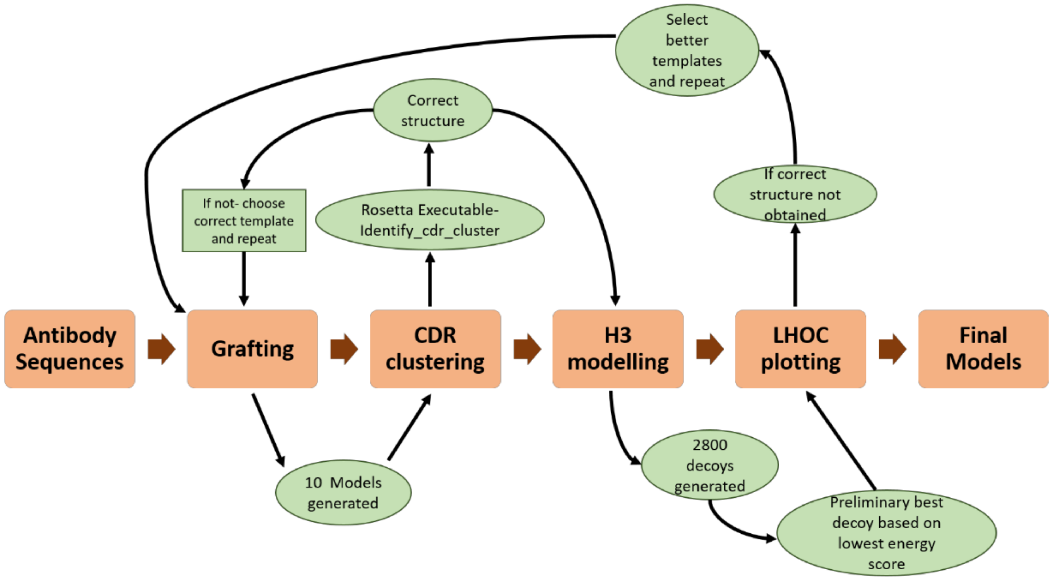

Figure.3.1: The complete representation of the protocol followed to generate the antibody models.

II. Modelling of the cognate human antibodies

The cognate antibodies were selected from a human antibody library by the members of Dr. Roger Johns' laboratory. They had initiated an antibody search using hresistin or hRELMβ to select S_CF_V binders from a phage display human S_CF_V library (Phage Display ScL-2 Library from Creative Biolabs) in two separate screens. 80 clones from each screen were initially chosen. Soluble ELISA was used to select 17 hresistin and 15 hRELMβ S_CF_V clones that bound to their respective targets positively. Then additional dose related ELISA was performed to determine which of these antibodies was specific to its intended target (hresistin or hRELMβ). These 32 S_CF_V fragments were subsequently made into full human IgG1 antibodies.

I modelled each of these 32 antibodies using RosettaAntibody protocol. After generating the final models, I determined CDR clusters of each of the CDR loops of the antibodies (Table.3.1 and Table.3.2).

Antibody	H1 cluster	H2 cluster	H3 cluster	L1 cluster	L2 cluster	L3 cluster
AntiRes-1	H1-13-1	H2-10-2	H3-9-2	L1-11-1	L2-8-1	L3-9-*cis*7-1
AntiRes-2	H1-13-1	H2-10-2	H3-9-1	L1-11-1	L2-8-1	L3-9-*cis*7-1
AntiRes-3	H1-13-1	H2-10-1	H3-9-1	L1-11-1	L2-8-1	L3-9-*cis*7-1
AntiRes-4	H1-13-1	H2-10-1	H3-9-1	L1-11-1	L2-8-1	L3-9-*cis*7-1
AntiRes-5	H1-13-1	H2-10-6	H3-9-1	L1-11-1	L2-8-1	L3-9-*cis*7-1
AntiRes-9	H1-13-1	H2-10-2	H3-9-2	L1-11-1	L2-8-1	L3-9-*cis*7-1
AntiRes-11	H1-13-1	H2-10-6	H3-9-2	L1-11-1	L2-8-1	L3-9-*cis*7-1
AntiRes-13	H1-13-1	H2-10-1	H3-9-2	L1-11-1	L2-8-1	L3-9-*cis*7-1
AntiRes-16	H1-13-1	H2-10-2	H3-9-2	L1-11-1	L2-8-1	L3-9-*cis*7-1

AntiRes-17	H1-13-1	H2-10-2	H3-9-1	L1-11-1	L2-8-1	L3-9-*cis*7-1
AntiRes-18	H1-13-1	H2-10-6	H3-9-1	L1-11-1	L2-8-1	L3-9-*cis*7-1
AntiRes-19	H1-13-1	H2-10-2	H3-9-1	L1-11-1	L2-8-1	L3-9-*cis*7-1
AntiRes-21	H1-13-1	H2-10-1	H3-9-1	L1-11-1	L2-8-1	L3-9-*cis*7-1
AntiRes-24	H1-13-1	H2-10-2	H3-9-1	L1-11-1	L2-8-1	L3-9-*cis*7-1
AntiRes-26	H1-13-1	H2-10-1	H3-9-1	L1-11-1	L2-8-1	L3-9-*cis*7-1
AntiRes-27	H1-13-1	H2-10-2	H3-9-1	L1-11-1	L2-8-1	L3-9-*cis*7-1
AntiRes-41	H1-13-1	H2-10-2	H3-9-1	L1-11-1	L2-8-1	L3-9-*cis*7-1

Table.3.1: The CDR cluster list of 17 hresistin S_CF_V antibody clones

Antibody	H1 cluster	H2 cluster	H3 cluster	L1 cluster	L2 cluster	L3 cluster
AntiRel-4	H1-13-1	H2-10-2	H3-9-2	L1-11-1	L2-8-1	L3-9-*cis*7-1
AntiRel-14	H1-13-1	H2-10-2	H3-9-1	L1-11-1	L2-8-1	L3-9-*cis*7-1
AntiRel-18	H1-13-1	H2-10-2	H3-9-2	L1-11-1	L2-8-1	L3-9-*cis*7-1
AntiRel-33	H1-13-1	H2-10-2	H3-9-2	L1-11-1	L2-8-1	L3-9-*cis*7-1
AntiRel-36	H1-13-1	H2-10-1	H3-9-1	L1-11-1	L2-8-1	L3-9-2
AntiRel-38	H1-13-1	H2-10-6	H3-9-2	L1-11-1	L2-8-1	L3-9-*cis*7-1
AntiRel-41	H1-13-1	H2-10-2	H3-9-1	L1-11-1	L2-8-1	L3-9-*cis*7-1
AntiRel-47	H1-13-1	H2-10-2	H3-9-2	L1-11-1	L2-8-1	L3-9-*cis*7-1
AntiRel-51	H1-13-1	H2-10-6	H3-9-2	L1-11-1	L2-8-1	L3-9-*cis*7-1
AntiRel-53	H1-13-1	H2-10-2	H3-9-2	L1-11-1	L2-8-1	L3-9-*cis*7-1
AntiRel-75	H1-13-1	H2-10-2	H3-9-2	L1-11-1	L2-8-1	L3-9-*cis*7-1
AntiRel-23	H1-13-1	H2-10-2	H3-9-1	L1-11-1	L2-8-1	L3-9-*cis*7-1

AntiRel-22	H1-13-1	H2-10-2	H3-9-2	L1-11-1	L2-8-1	L3-9-*cis*7-1
AntiRel-28	H1-13-1	H2-10-2	H3-9-2	L1-11-1	L2-8-1	L3-9-*cis*7-1
AntiRel-31	H1-13-1	H2-10-2	H3-9-2	L1-11-1	L2-8-1	L3-9-*cis*7-1

Table.3.2: The CDR cluster list of 15 hRELMβ S_CF_V antibody clones

Predicting the three-dimensional structure is a crucial step in improving the affinity, stability and suitability of these antibodies as therapeutics. The V_H and V_L domains of the antibodies are highly conserved and the CDR loops have small discrete set of main-chain conformations known as the canonical structures. These CDR clusters are based on the classification of antibody CDR loop conformations[51-53]. The nomenclature of the classification is CDR-loop length-cis/trans conformation-cluster number. I classified the cluster of each CDR loop using the North CDR clustering library[51-53]. This step was necessary, as I could check whether the templates with the most similarities in the sequence were used initially in the grafting step of RosettaAntibody protocol. In majority of the antibodies, the CDR loop conformations matched with the most populous CDR clusters. In a few cases the H2 CDR loop conformation preferred a rare CDR cluster (H2-10-6) since the H2 CDR loop sequence matched the consensus sequence of the cluster suggests that the rare cluster chosen was appropriate.

III. Structural analysis of the cognate antibodies

In experimental studies, the antibody AntiRes-13 showed the highest binding affinity towards hresistin and hRELMβ. Apart from this AntiRes-2, AntiRes-

3, AntiRes-9, AntiRes-11 and AntiRes-41 also showed good binding affinity. For further discussion, I will focus on these top six antibodies.

After I generated the final 2800 decoys, V_H-V_L orientation of each of the antibodies are checked whether they match observed distributions of the orientations of all the antibodies of the crystal antibody structures found in the PDB. I generated four plots based on the LHOC metrices which are interdomain distance, heavy opening angle, light opening angle and packing angle. Each plot shows the native distribution of V_L–V_H orientations (grey), the orientations sampled by Rosetta (black line), the top 10 models (labeled diamonds) and the 10 different template structures (labelled dots) used during grafting. From the LHOC plots of AntiRes-13 (Figure.3.2), I observed the top 10 models were within the native distribution V_H-V_L orientation. Similarly, for antibodies AntiRes-3 (Figure.3.3), AntiRes-2, AntiRes-9, and AntiRes-11 LHOC plots showed that my models were predicted accurately. Overall all my 32 antibody models were within native distributions.

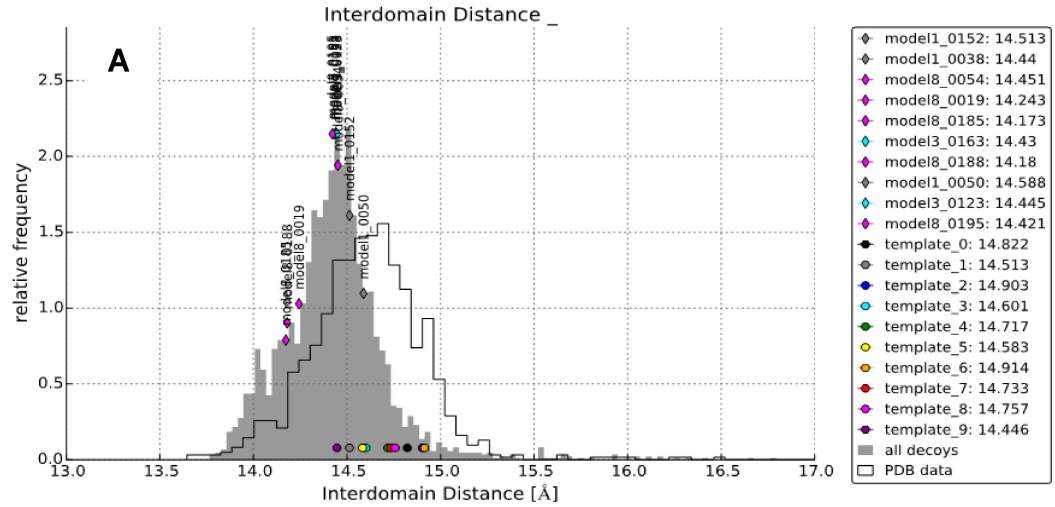
A
Interdomain Distance _
relative frequency
Interdomain Distance [Å]
model1_0152: 14.513
model1_0038: 14.44
model8_0054: 14.451
model8_0019: 14.243
model8_0185: 14.173
model3_0163: 14.43
model8_0188: 14.18
model1_0050: 14.588
model3_0123: 14.445
model8_0195: 14.421
template_0: 14.822
template_1: 14.513
template_2: 14.903
template_3: 14.601
template_4: 14.717
template_5: 14.583
template_6: 14.914
template_7: 14.733
template_8: 14.757
template_9: 14.446
all decoys
PDB data

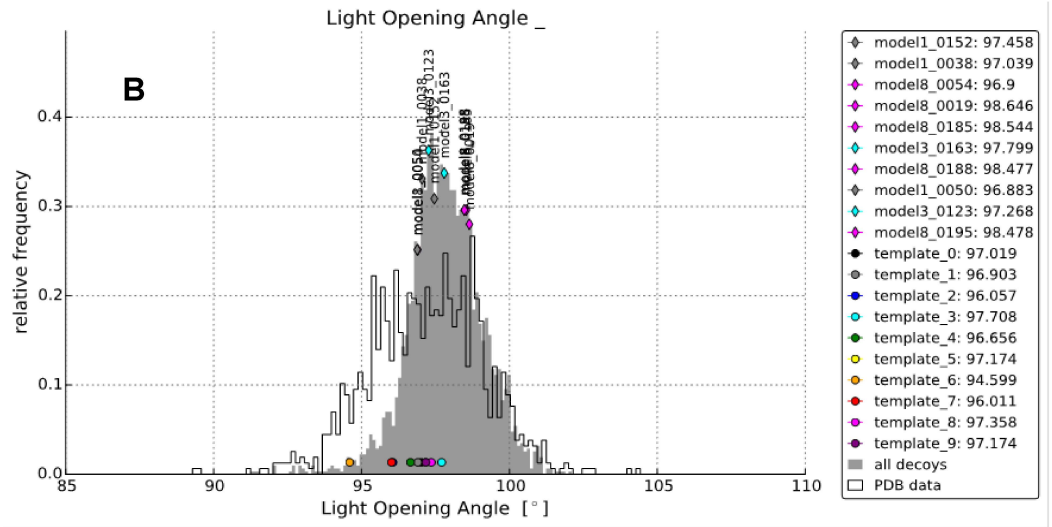
B
Light Opening Angle _
relative frequency
Light Opening Angle [°]
model1_0152: 97.458
model1_0038: 97.039
model8_0054: 96.9
model8_0019: 98.646
model8_0185: 98.544
model3_0163: 97.799
model8_0188: 98.477
model1_0050: 96.883
model3_0123: 97.268
model8_0195: 98.478
template_0: 97.019
template_1: 96.903
template_2: 96.057
template_3: 97.708
template_4: 96.656
template_5: 97.174
template_6: 94.599
template_7: 96.011
template_8: 97.358
template_9: 97.174
all decoys
PDB data

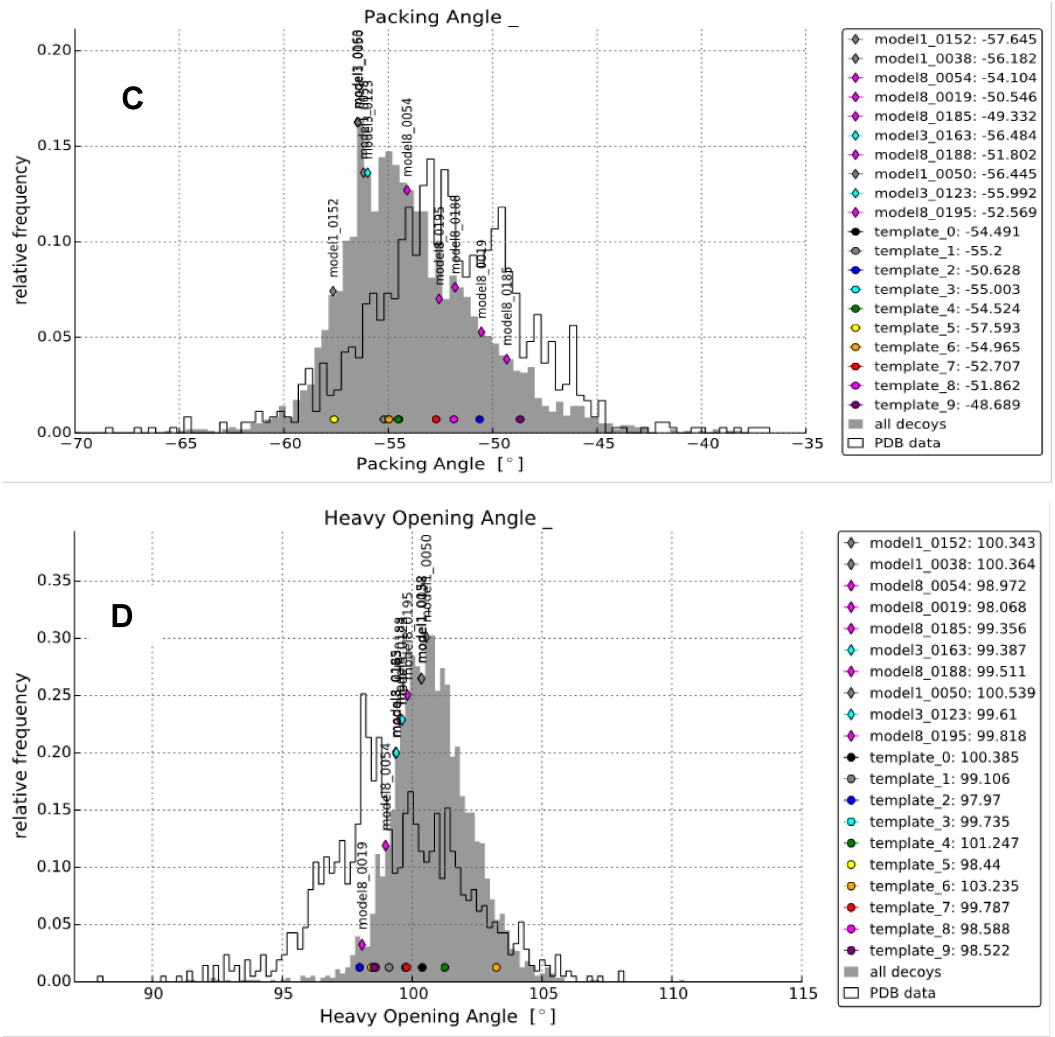

Figure.3.2: The LHOC subplots of antibody AntiRes-13

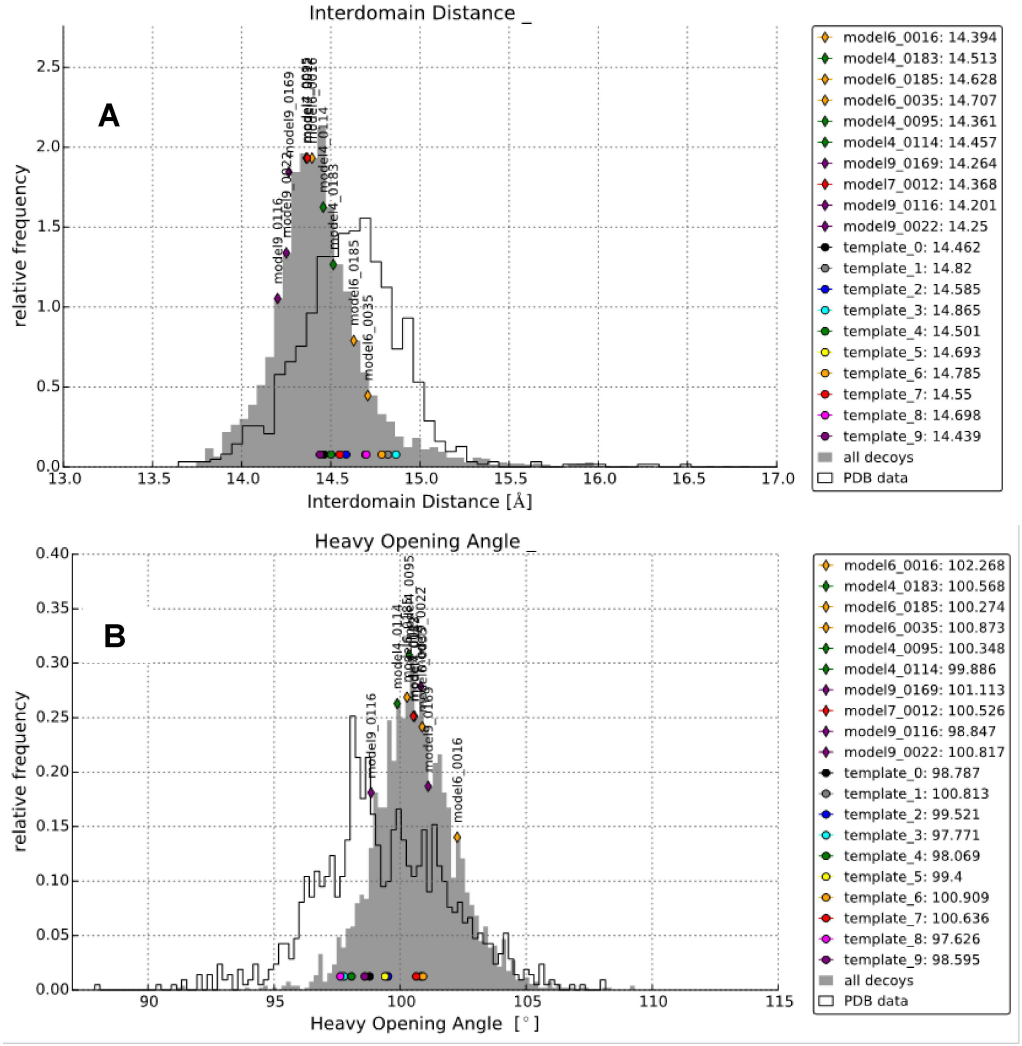
A
Interdomain Distance _
relative frequency
Interdomain Distance [Å]
model6_0016: 14.394
model4_0183: 14.513
model6_0185: 14.628
model6_0035: 14.707
model4_0095: 14.361
model4_0114: 14.457
model9_0169: 14.264
model7_0012: 14.368
model9_0116: 14.201
model9_0022: 14.25
template_0: 14.462
template_1: 14.82
template_2: 14.585
template_3: 14.865
template_4: 14.501
template_5: 14.693
template_6: 14.785
template_7: 14.55
template_8: 14.698
template_9: 14.439
all decoys
PDB data
B
Heavy Opening Angle _
relative frequency
Heavy Opening Angle [°]
model6_0016: 102.268
model4_0183: 100.568
model6_0185: 100.274
model6_0035: 100.873
model4_0095: 100.348
model4_0114: 99.886
model9_0169: 101.113
model7_0012: 100.526
model9_0116: 98.847
model9_0022: 100.817
template_0: 98.787
template_1: 100.813
template_2: 99.521
template_3: 97.771
template_4: 98.069
template_5: 99.4
template_6: 100.909
template_7: 100.636
template_8: 97.626
template_9: 98.595
all decoys
PDB data

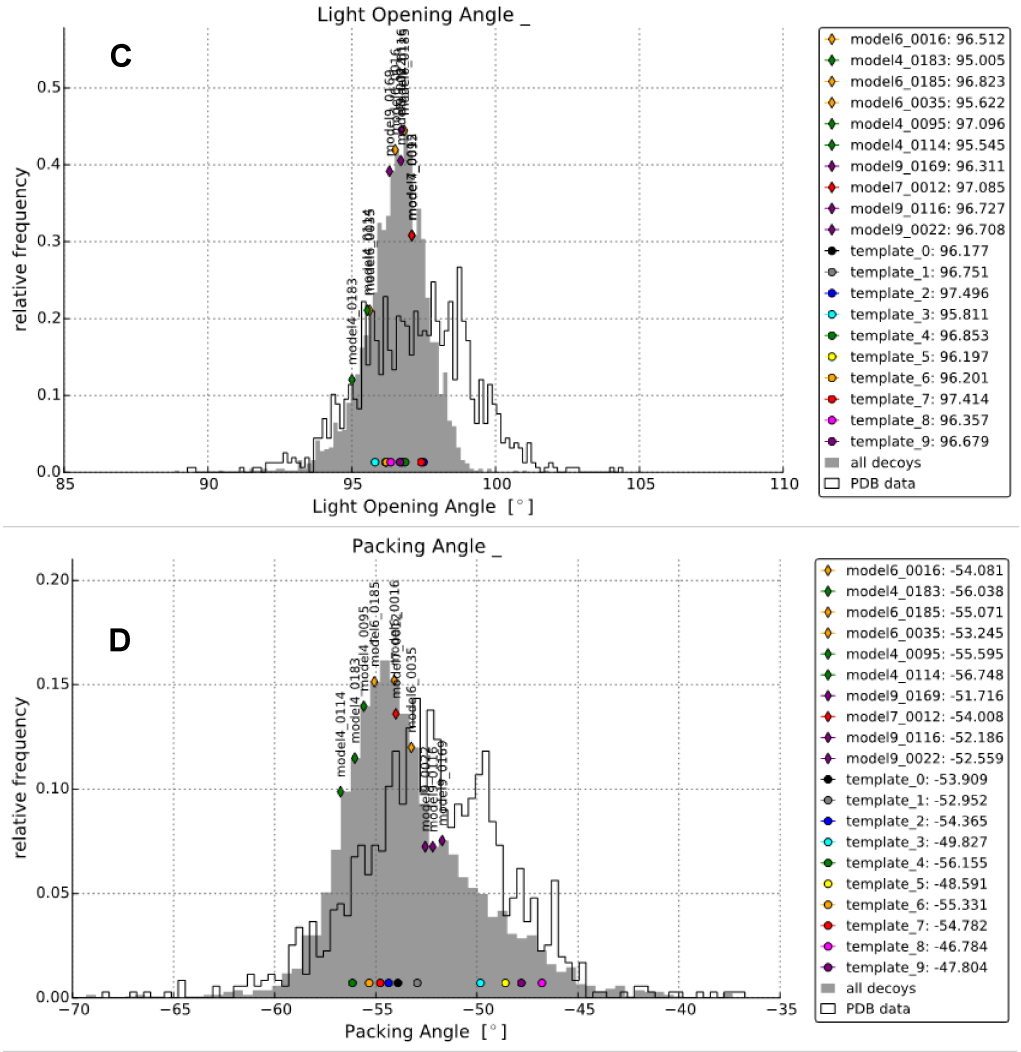

Figure.3.3:The LHOC subplots of antibody AntiRes-3

After checking all the LHOC plots, I selected the final three-dimensional structures of the antibodies based on the lowest Rosetta energy score. The typical structure of the antibodies is shown in Figure.3.4. I also calculated the surface charge distribution of each of the antibodies. From the calculations, the binding pockets of each of the antibodies have strong electrostatic

potential. The presence of these strong electrostatic potentials will have an effect of the binding capabilities of the antibodies.

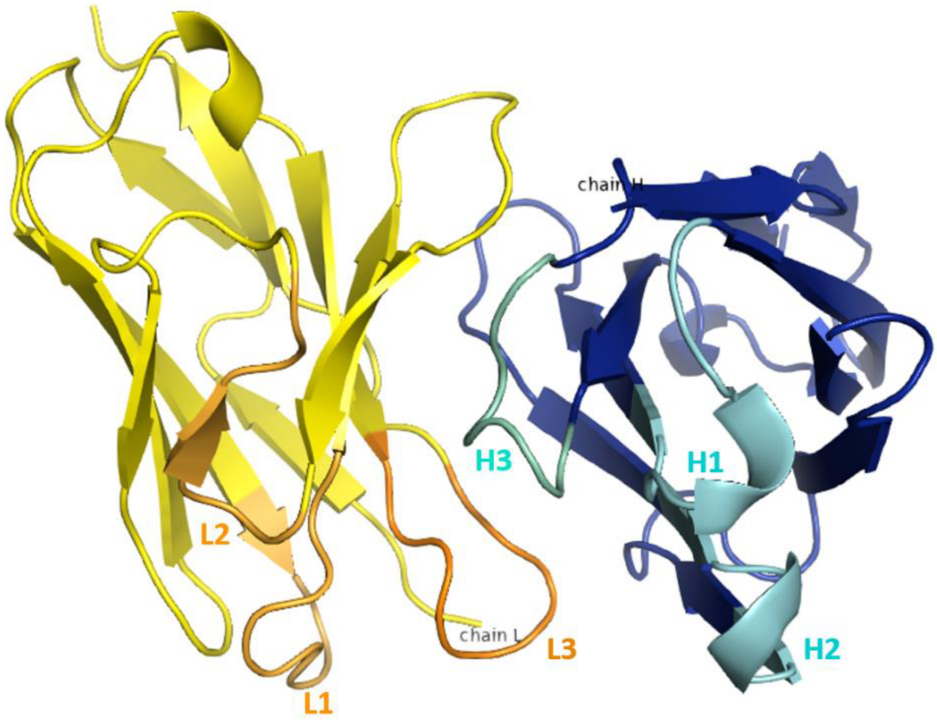

Figure.3.4: Typical structure of the antibody highlighting the light region (yellow), heavy region (navy blue), light chain CDR loops (orange) and heavy chin CDR loops(cyan)

CHAPTER IV

ANTIBODY-ANTIGEN DOCKING RESULTS

I. Overview

Immunoprecipitation experiments showed us that the antibodies bind to hresistin and hRELMβ but the binding regions couldn't be determined experimentally. To predict these binding regions and hence find the epitopes regions, I used ClusPro software package and RosettaSnugDock protocol. Using ClusPro I performed global docking to determine all possible docking conformations of the antibody-antigen complex[54-59]. From all the candidate docking conformations, I selected the top 10 poses and used them as starting points for local docking. To perform local docking, I used RosettaSnugDock protocol[60]. From RosettaSnugDock, I generated 1000 decoys for each of the 10 starting poses. I selected the lowest energy model, by the interface energy, whose interface RMSD falls within a range of 10Å of the local starting structures. I used this lowest energy model as a reference structure and recalculated all the RMSDs of the rest of the decoys to the reference state. This allows me to view the energy surface near the reference structure to see if it forms an energy funnel. This determines whether our chosen docked pose is the true docked state. If its not, then the steps are repeated till I determine the most likely docked state. After the final docked state is determined, I examine the putative binding site on the target antigen based on the interaction between the CDR loop residues and the antigen residues at the interface. Figure.4.1 shows the overall flowchart of the methodology followed.

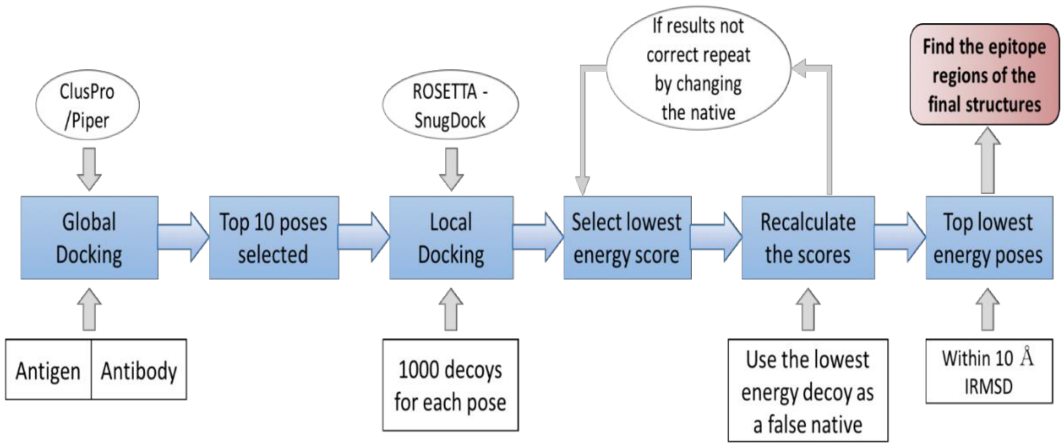

Figure.4.1: The flowchart shows the complete computational methodology applied for antibody-antigen docking

II. Global Docking Results

Based on experimental results performed in the John's lab, it was decided to explore antibody docking to the monomer state of the proteins. So, for my antibody-antigen docking, I selected the monomer state of both hresistin + hRELMβ and docked them with the antibodies. Initially to determine the docked conformation between the antibody and antigen, I used ClusPro software package[54-59]. ClusPro software developed in the Boston University performs protein-protein docking. It determines the interface between the proteins by calculating intermolecular forces and shape complementarity features. Different modes are used for different protein-protein docking

interactions. I used the antibody mode for global docking of my antibody-antigen systems to restrict the antibody interaction to its CDRs. ClusPro determines the best possible docking conformations of the antibody-antigen complex[59]. The top 10 docked conformations are selected. These top 10 conformations are then used as starting points for locking docking calculations.

III. Local Docking Results

Using the ClusPro results as starting points, I used RosettaSnugDock protocol to generate 1000 decoys, for each of the top 10 docked conformations. From the local docking results, I plotted interface energy scores vs interface RMSD for all the 10,000 decoys(Figure.4.2). From the plot, I selected models which had the lowest interface energy within a range of 10Å interface RMSD. I used the lowest energy model as a reference structure docked state and recalculated all the RMSDs of the remaining decoys. This recalculation is a crucial step in determining whether the chosen lowest energy model, is the most likely docked state of the antibody-antigen complex.

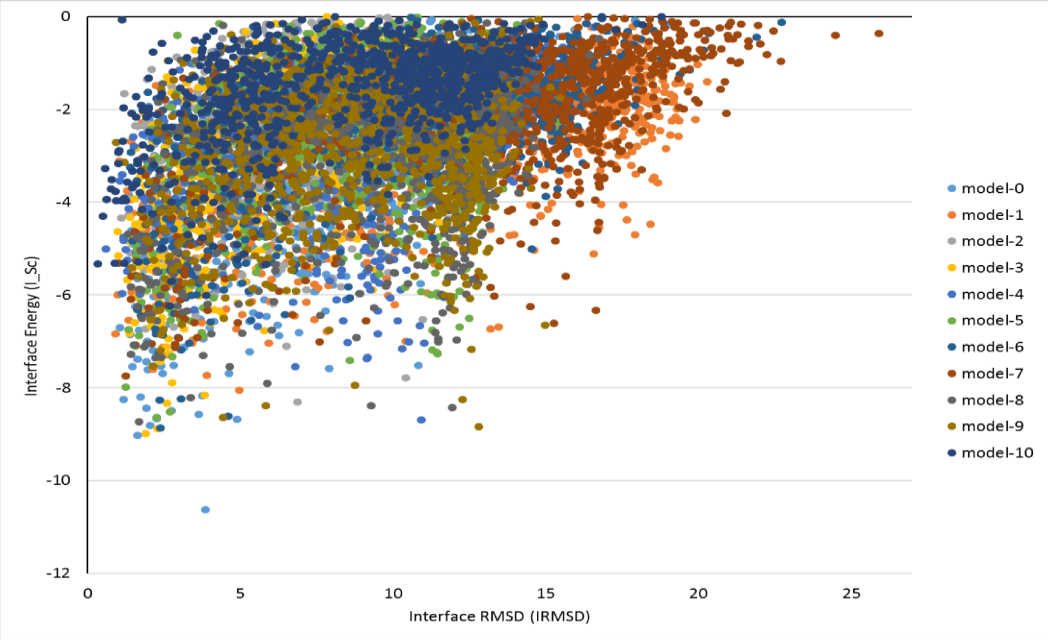

Figure.4.2: Typical energy funnel plot of all the 10000 decoys generated from RosettaSnugDock protocol using the top 10 docking models from ClusPro as starting positions.

From the immunoprecipitation experiments, the antibody AntiRes-13, showed very strong binding affinity to hresistin and hRELMβ. Using ClusPro and RosettaSnugDock, I generated many possible docking conformations of AntiRes-13 with hresistin. I selected the lowest energy model and used it as a refereence structure and recalculated all the RMSDs (Figure.4.3).

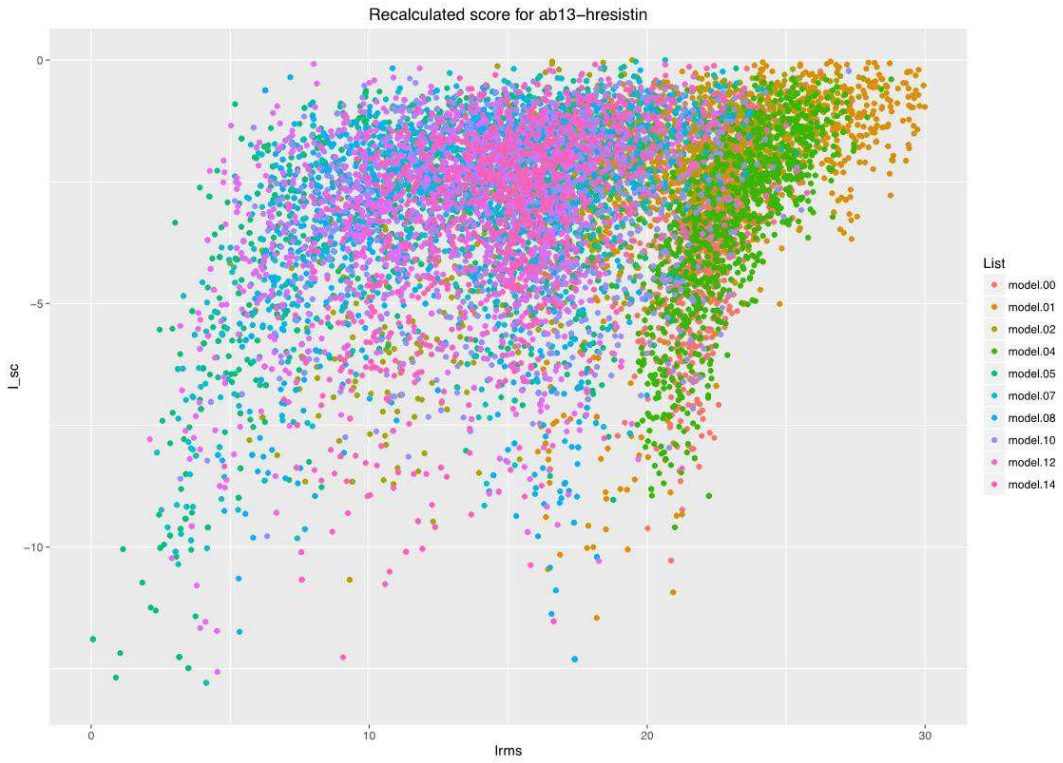

Figure.4.3: Docking results of antibody AntiRes-13 with hresistin. The energy funnel plot of all the recalculated decoys based on the lowest energy model as a native structure shows convergence.

From the plots, a good energy funnel was observed towards the reference structure. To check the quality of my docking results, I performed the bootstrap statistical analysis (N_5 analysis)[62]. Bootstrap statistical analyses are model-independent analyses which approximate statistic variables such as mean, standard deviation, and test statistics without making assumptions about the distribution of the underlying data. From this analysis a docking success criteria of μ (N_5) $\geq$2.5 and $P_{success}$ $\geq$0.3 is set. My docking runs fell within this range with μ (N_5) = 4.76 and $P_{success}$ = 0.947 suggesting my data are successful and well converged. I compared the structures of the lowest energy models within a range of 5Å interface RMSD and -10 kcal/mol interface energy score. All the structures within this range converged to

similar docked conformation. I chose the final docked prediction of AntiRes-13 binding to hresistin (Figure.4.4) where AntiRes-13 binds strongly to the head region of hresistin. I determined the potential epitope region by calculating the residues interacting between the antibody and the antigen. Residues39L+40A+41T+42C+58G+59S+76D+77W+78T+79G+80A+72C+73A of hresistin bind to the antibody AntiRes-13 (Figure.4.4) on the low energy models.

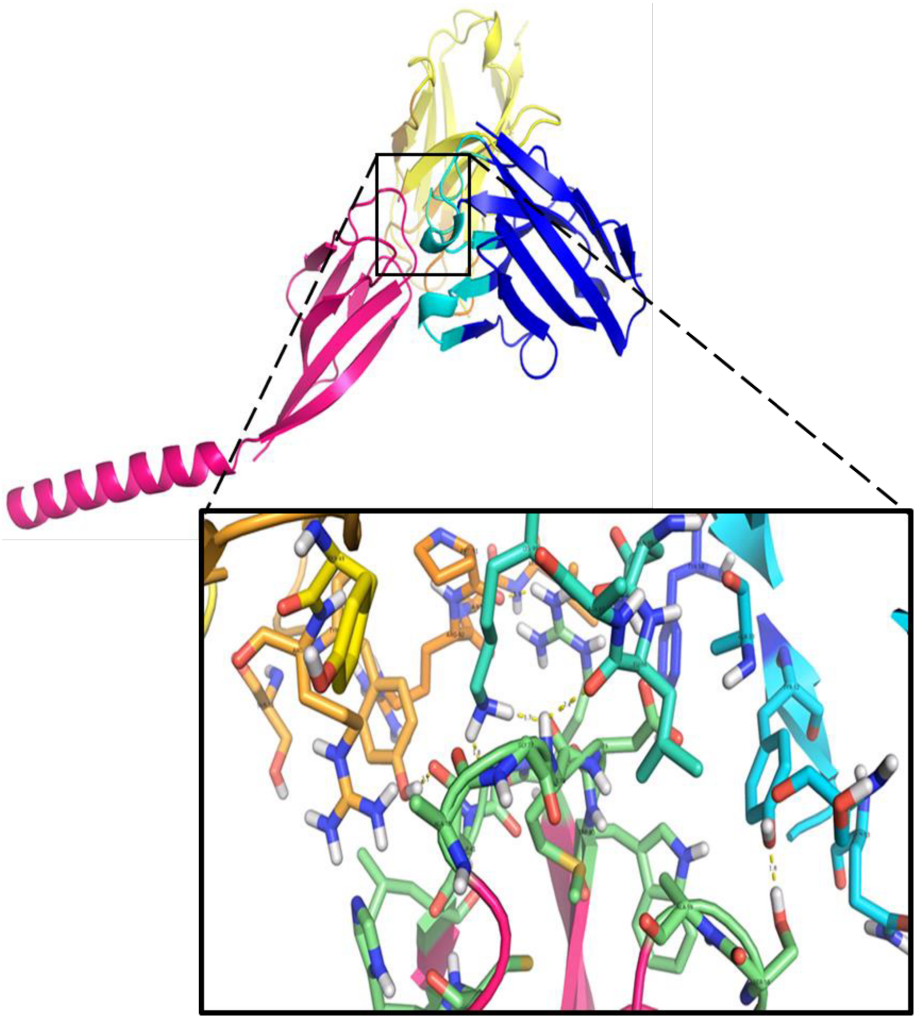

Figure.4.4: The final docked conformation of AntiRes-13 with hresistin (deep pink). The enlarged image of the binding interface shows the epitope region (pale green) interacting with light chain CDR loops (orange) and the heavy chain CDR loops(cyan).

I repeated the same procedure for AntiRes-13 with hRELMβ, and determined the final recalculated energy funnel plot (Figure.4.5). From the plot, I observed that a good convergence wasn't observed after performing the bootstrap statistical analysis with $P_{success} = 0.21$ even though my chosen native structure was the lowest energy model. Only the decoys similar to the lowest energy model in-terms of the initial starting position as determined by ClusPro converged well.

Figure.4.5: Docking results of antibody AntiRes-13 with hRELMβ. The energy funnel plot of all the recalculated decoys based on the lowest energy model as a native structure shows convergence of only those decoys which had same starting pose as the native structure.

I determined the final docked state and its epitope region (Figure.4.6). I observed that AntiRes-13 docks to the tail region of hRELMβ rather than the head. The epitope region of hRELMβ were determined as

36K+37D+38V+58V+59K+61Q+63R+69A+71M+72A+73V+74T+75G+76C+77A.

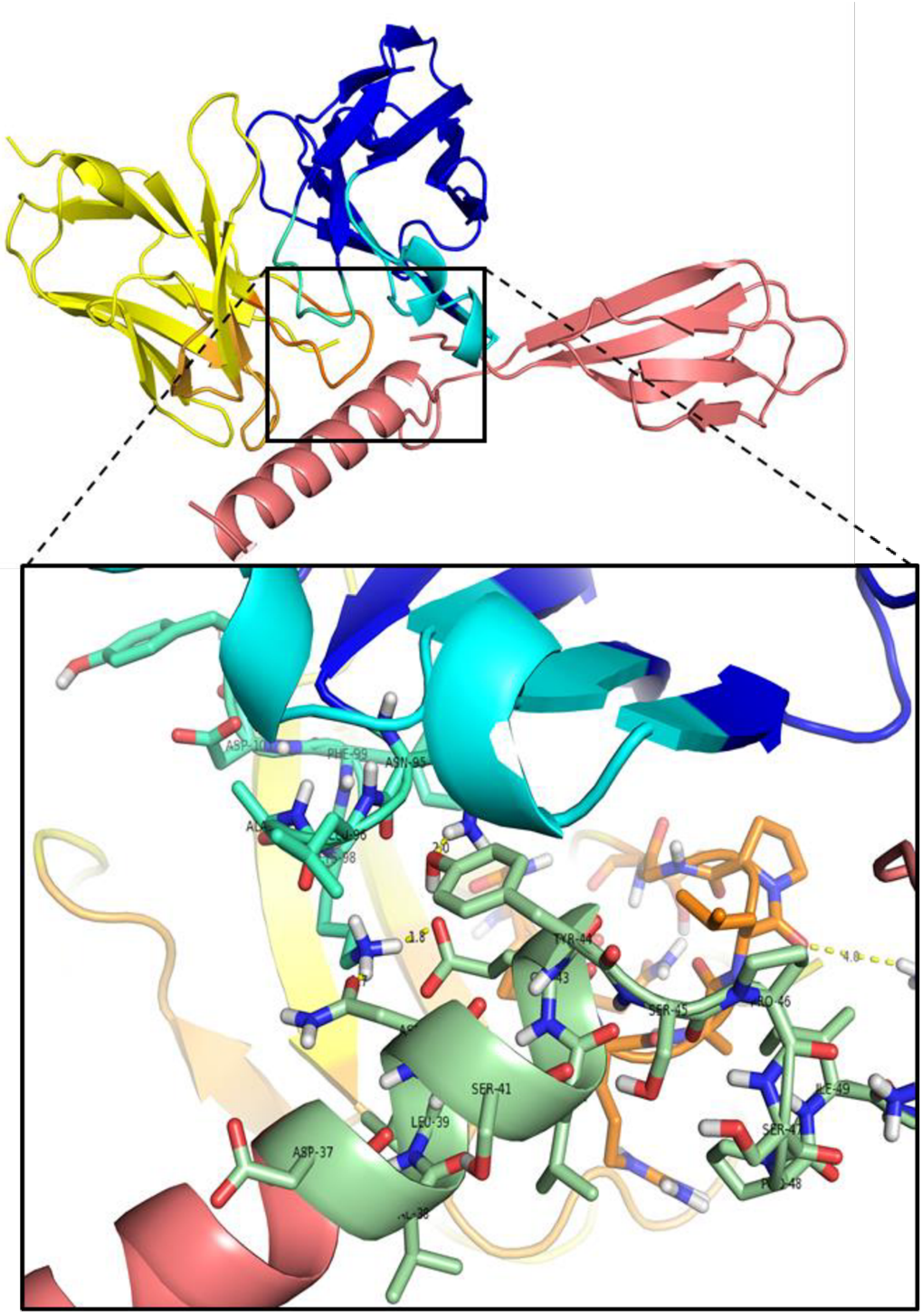

Figure.4.6: The final docked conformation of AntiRes-13 with hRELMβ (salmon). The enlarged image of the binding interface shows the epitope region (pale green) interacting with light chain CDR loops (orange) and the heavy chain CDR loops(cyan).

The docking results of AntiRes-13 with hRELMβ contrasted with hresistin. This was unexpected because both hresistin and hRELMβ have a strong homology in the head region which I had discussed in the previous chapters. From the docking results, I could determine that RosettaSnugDock was not able to determine a good docked pose. This may be due to the strong hydrophobic regions on the tail, and Rosetta prefers hydrophobic interactions between residues possibly more. Due to this the true docked state couldn't be determined.

When I docked AntiRes-2 to hresistin and hRELMβ, I observed similar results as AntiRes-13. From the recalculated energy funnels of AntiRes-2 with hresistin (Figure.4.7) and hRELMβ(Figure.4.8), a strong convergence and deep energy funnel was observed in hresistin, while it wasn't observed in hRELMβ. In case of AntiRes-2 binding to hRELMβ, an alternate conformation was preferred rather than the reference structure. This is observed in the energy funnel plots also as the decoys tend to converge at a different position.

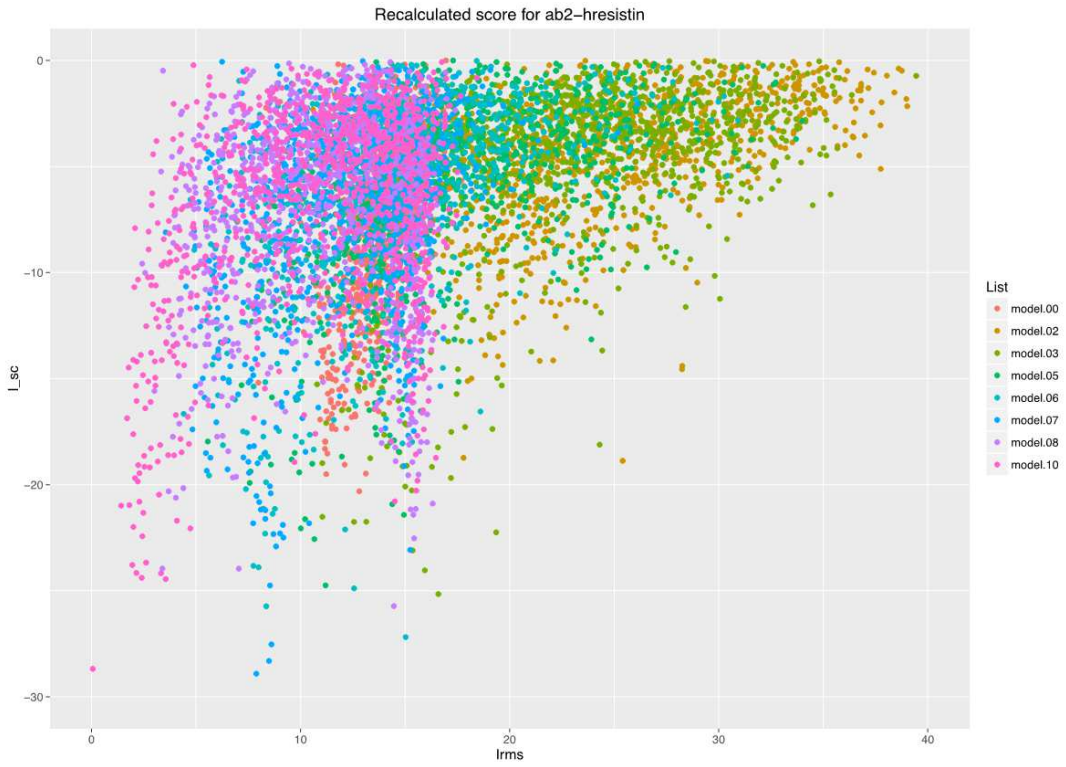

Figure.4.7: Docking results of antibody AntiRes-2 with hresistin. The energy funnel plot of all the recalculated decoys based on the lowest energy model as a native structure shows convergence.

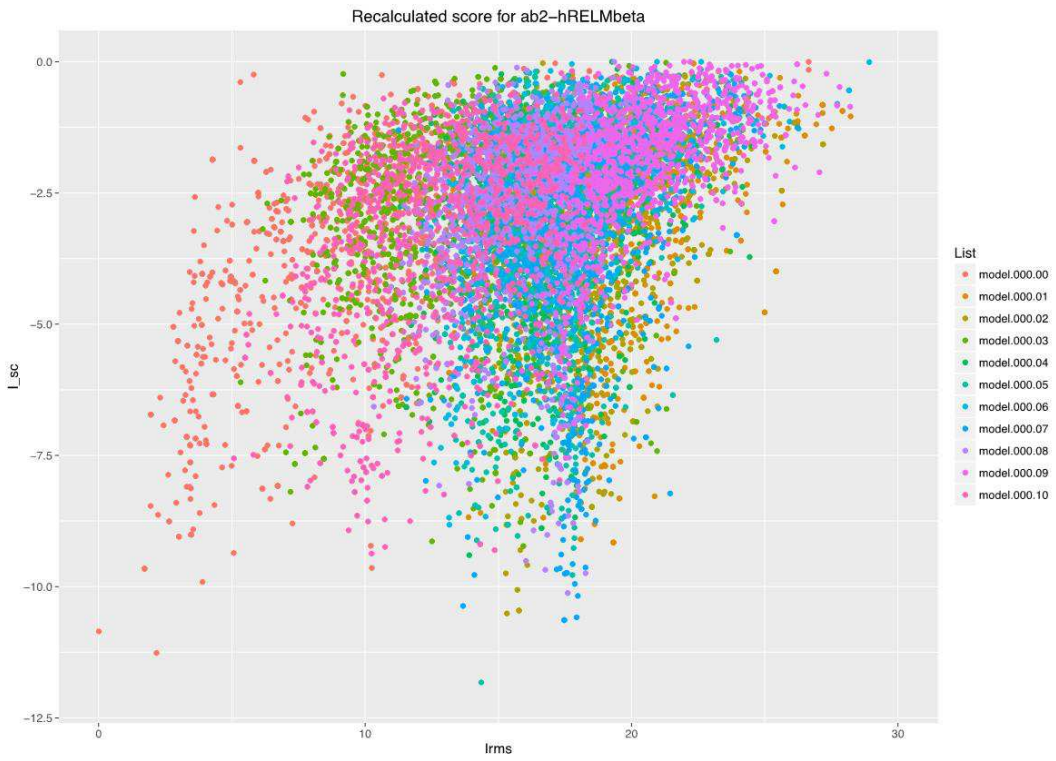

Figure.4.8: Docking results of antibody AntiRes-13 with hRELMβ. The energy funnel plot of all the recalculated decoys based on the lowest energy model as a reference structure shows convergence of only those decoys which had same starting pose as the native structure.

The final docked state for AntiRes-2 with both the protein were determined and their epitope regions calculated. AntiRes-2 docks best to the head of hresistin (Figure.4.9) whereas it docks best to the tail of hRELMβ (Figure.4.10). The docking results for AntiRes-2 to hRELMβ are ambiguous.

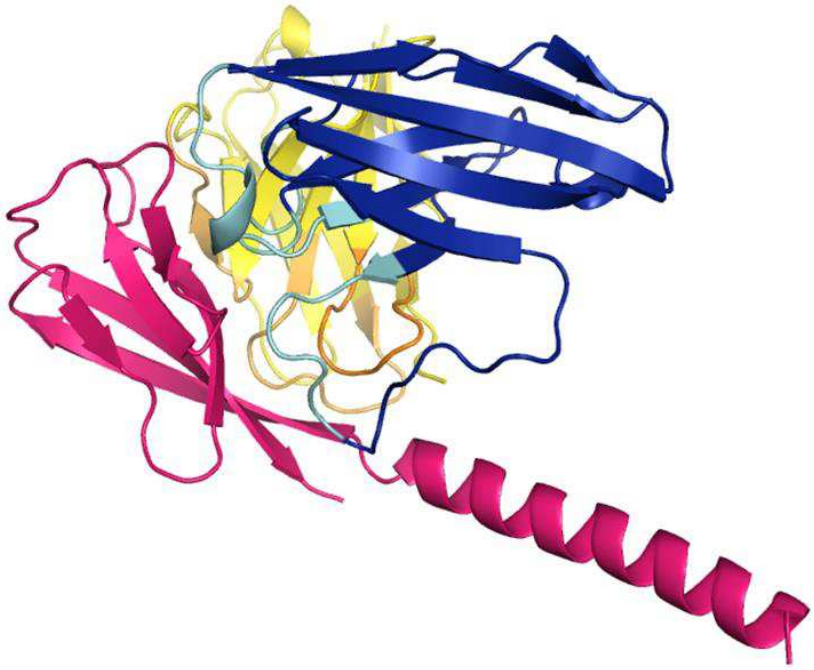

Figure.4.9: Final docked state of antibody AntiRes-2 and hresistin (deep pink)

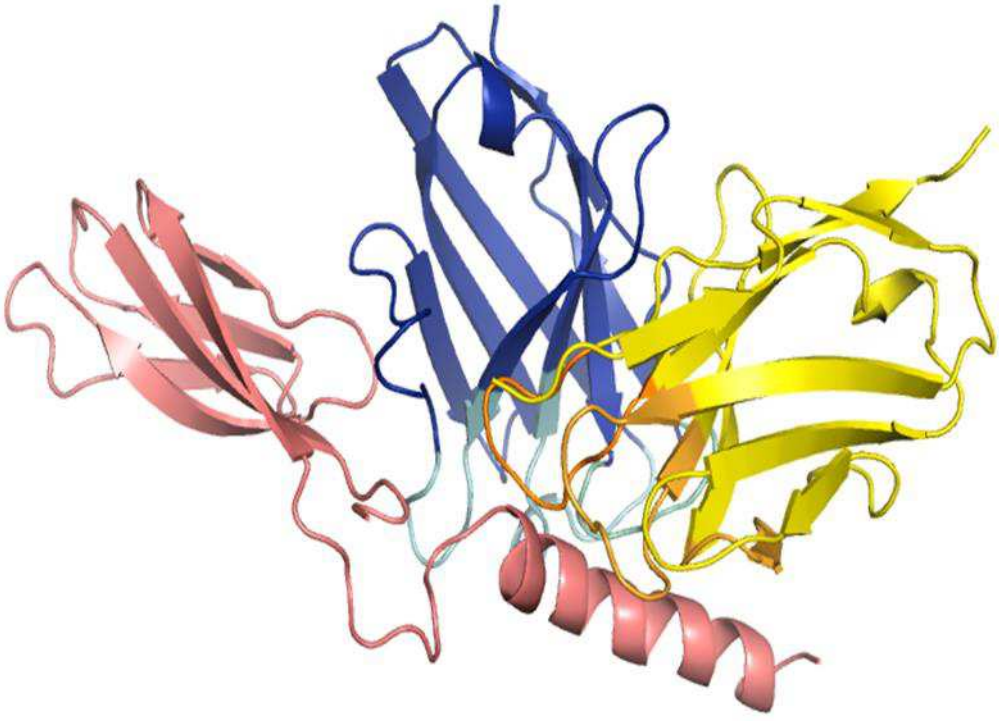

Figure.4.10: Final docked state of antibody AntiRes-2 with hRELMβ(salmon)

When I docked AntiRes-3 with hresistin and hRELMβ, I observed poor docking funnels after the recalculation of the energy scores both in hresistin (Figure.4.11) and hRELMβ (Figure.4.12). I observed poor energy funnels and the convergence wasn't good at all. When I determined the final docked state of AntiRes-3 with hresistin (Figure.4.13) and hRELMβ(Figure.4.14), the antibody binds to the tail regions of both the antigens. I couldn't determine whether these were the likely docking positions or these positions were selected by Rosetta due to preference of hydrophobic interactions.

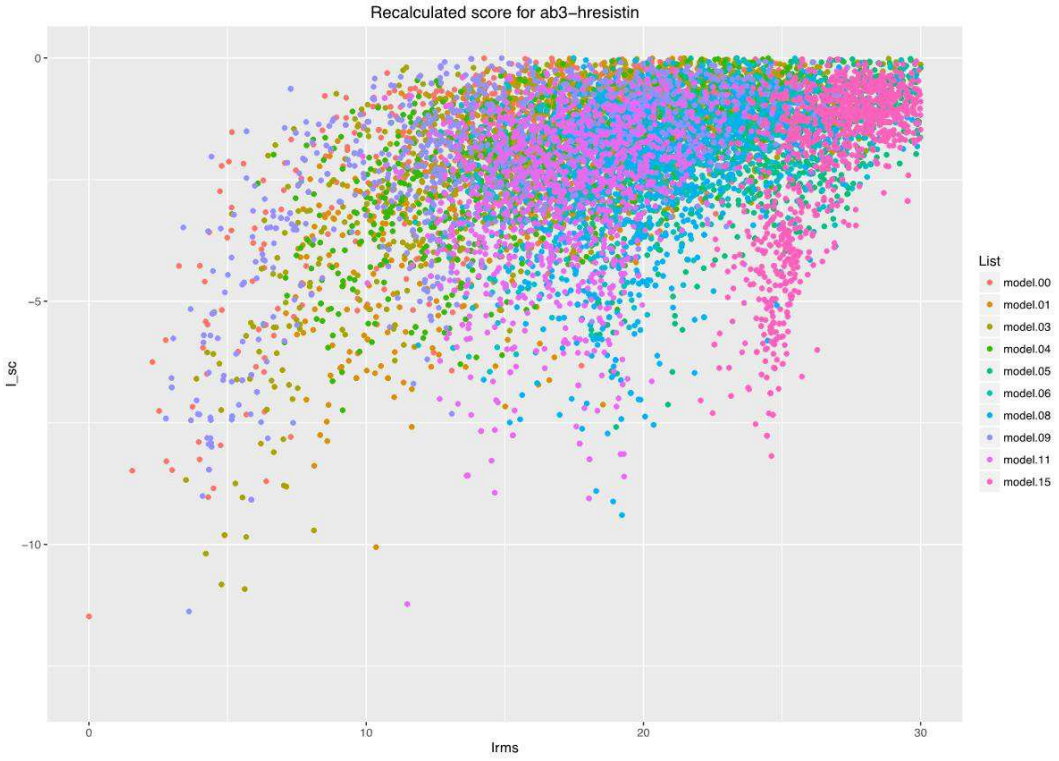

Figure.4.11: Docking results for AntiRes-3 with hresistin showing energy funnel formation with low convergence.

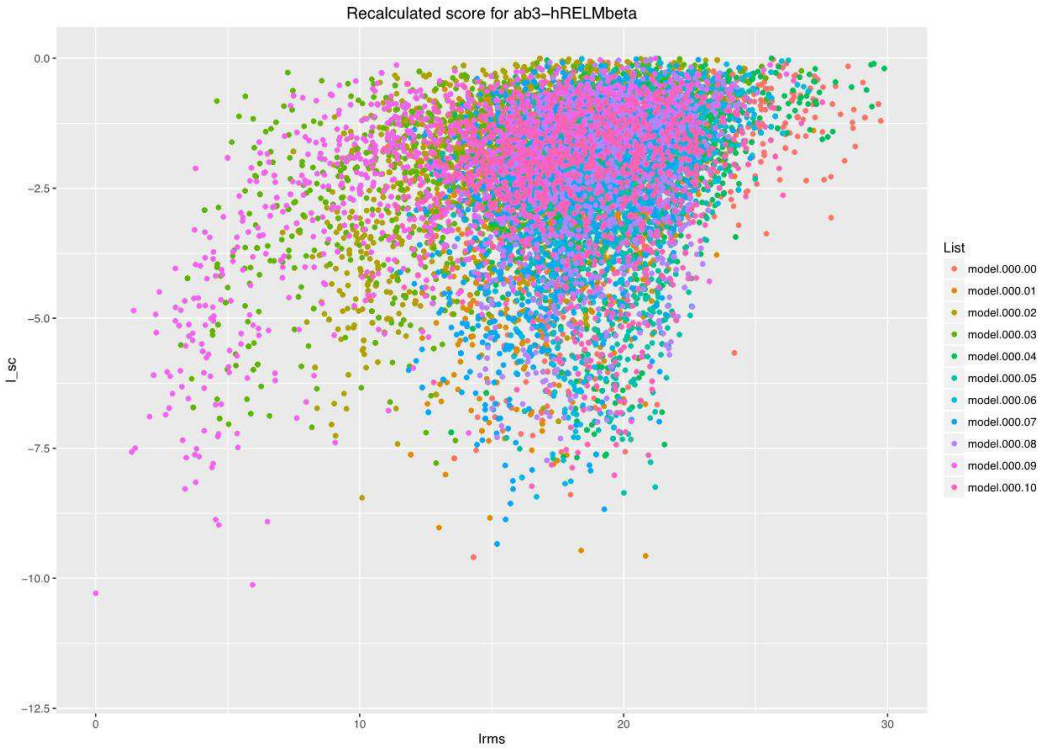

Figure.4.12: Docking results of AntiRes-3 with hRELMβ with poor energy funnel formation with very low convergence

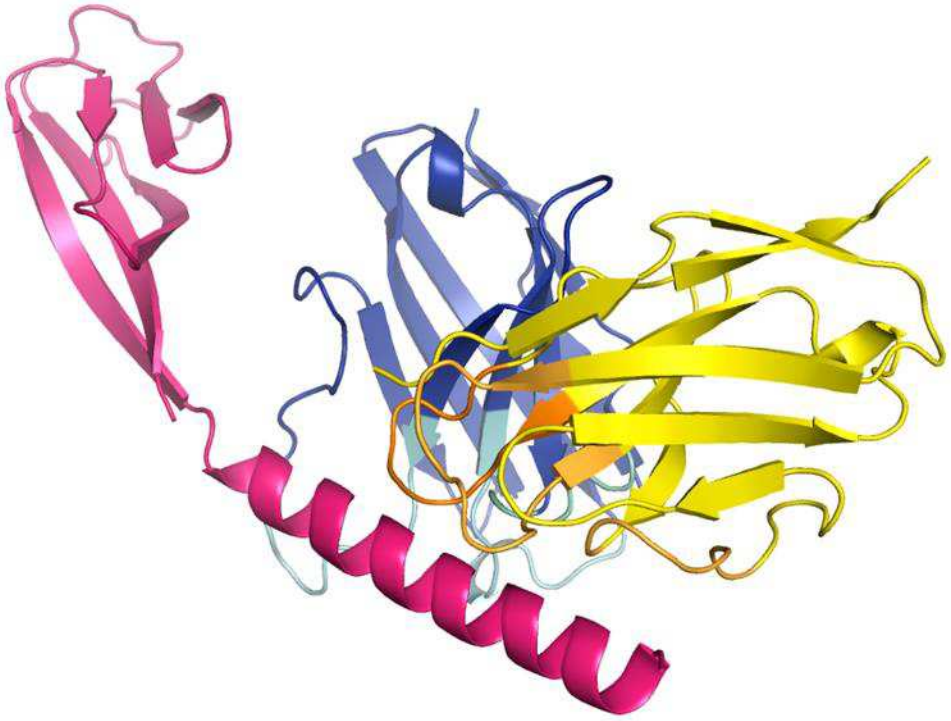

Figure.4.13: Final docked state of AntiRes-3 with hresistin (deep pink)

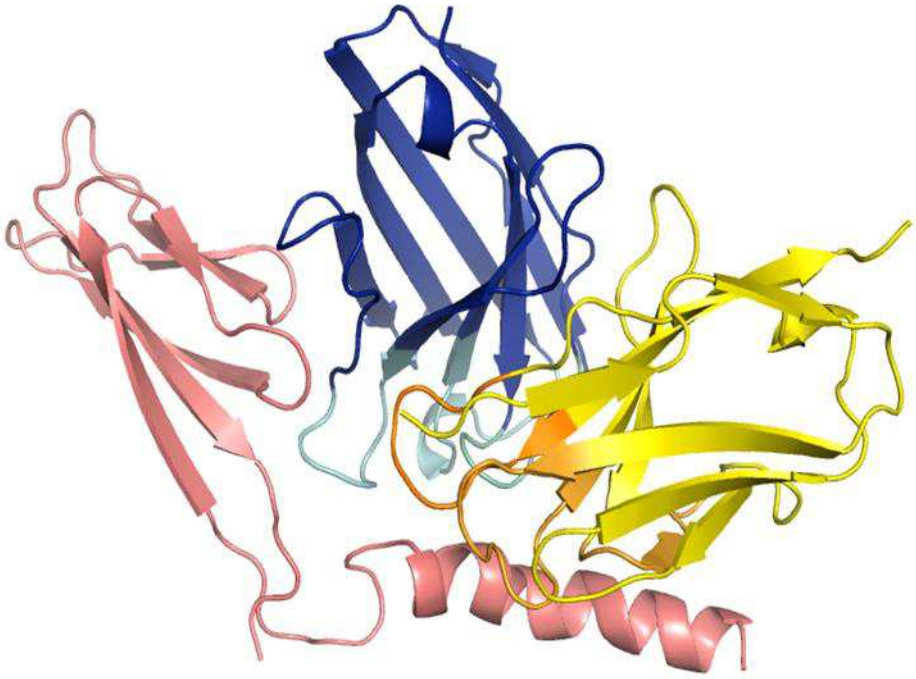

Figure.4.14: Final docked state of AntiRes-3 with hRELMβ(salmon)

Docking antibody AntiRes-9 with hresistin and hRELMβ showed positive results. Computationally the prediction of the final docked state for AntiRes-9 binding with hRELMβ showed much better results than hresistin. This is because the native structure I had chosen for recalculation had the lowest energy state (Figure.4.15). It also had a good energy difference with the other decoys also. AntiRes-9 bind to the head region for both hresistin(Figure.4.16) and hRELMβ(Figure.4.17). They bound to the same epitope regions.

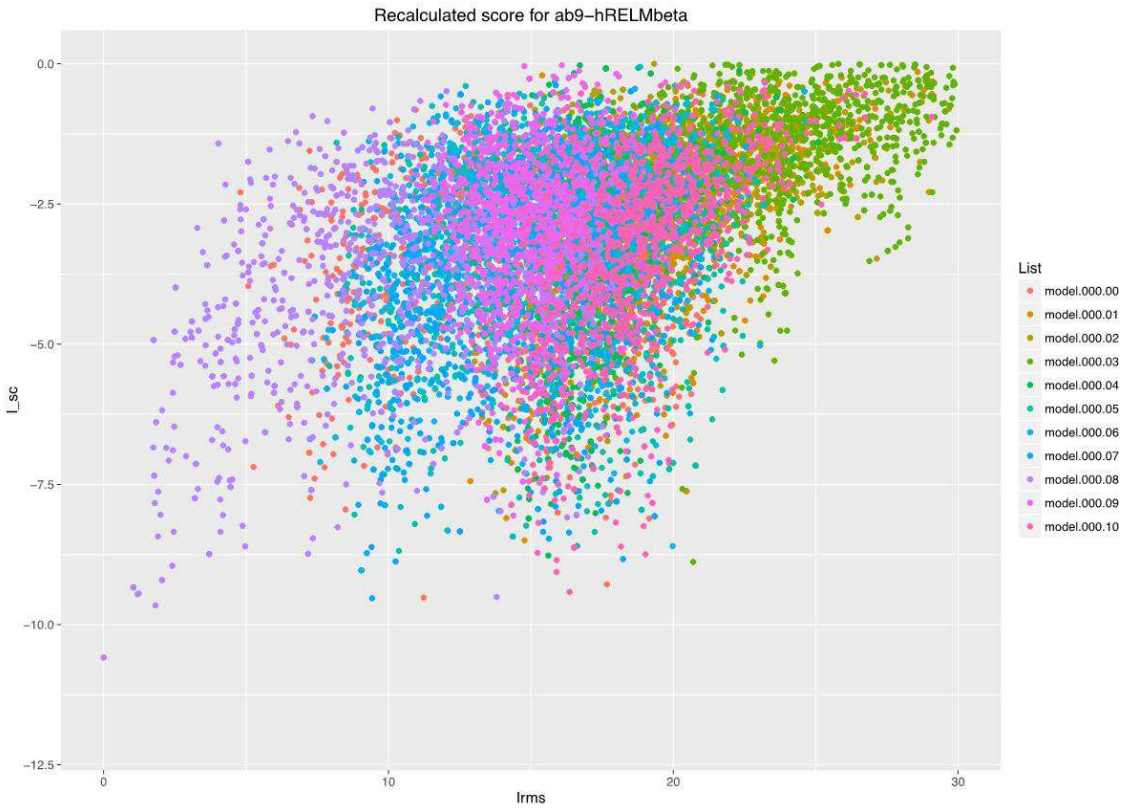

Figure.4.15: The energy funnel of AntiRes-9 docking with hRELMβ shows the native structure chosen may be the true binding state as the energy gap compared with other decoys is strong.

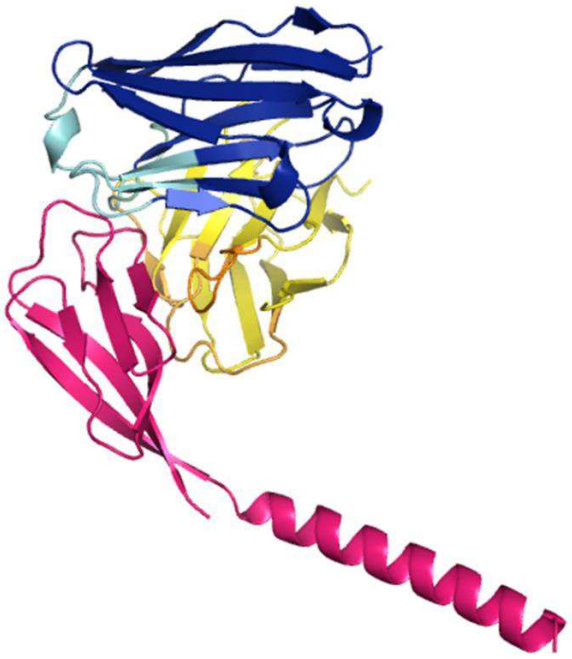

Figure.4.16: The final docked state of AntiRes-9 with hresistin (deep pink)

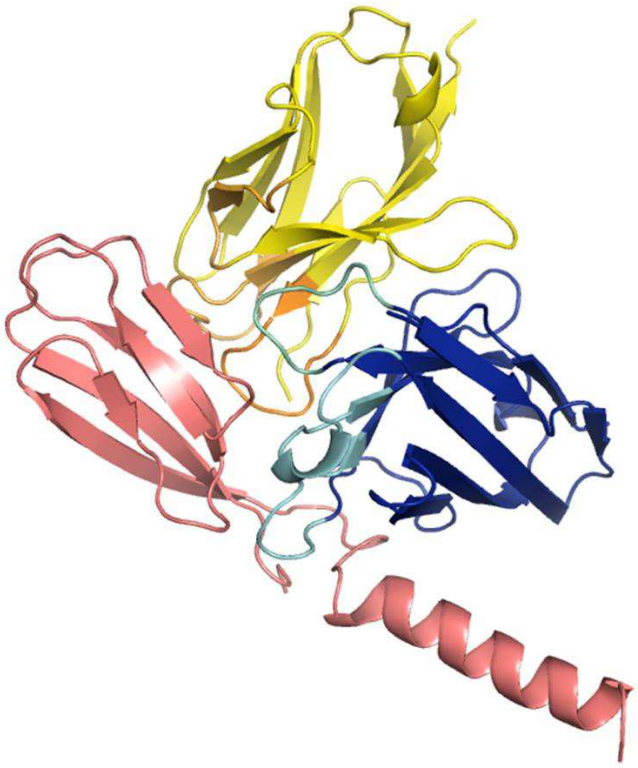

Figure.4.17:The final docked state of AntiRes-9 with hRELM(salmon)

Docking AntiRes-11 with hresistin and hRELMβ, produced the best results till now. The antibody docks strongly to the head region of both the proteins. After recalculating the energy scores, in both cases strong convergence was seen towards the lowest energy structure and it had a strong energy difference compared to the other decoys (Figure.4.18). The results suggest that computationally I could predict the true docked state of the antibody with the both the proteins(Figure.4.19). I calculated the epitope regions also in both the cases.

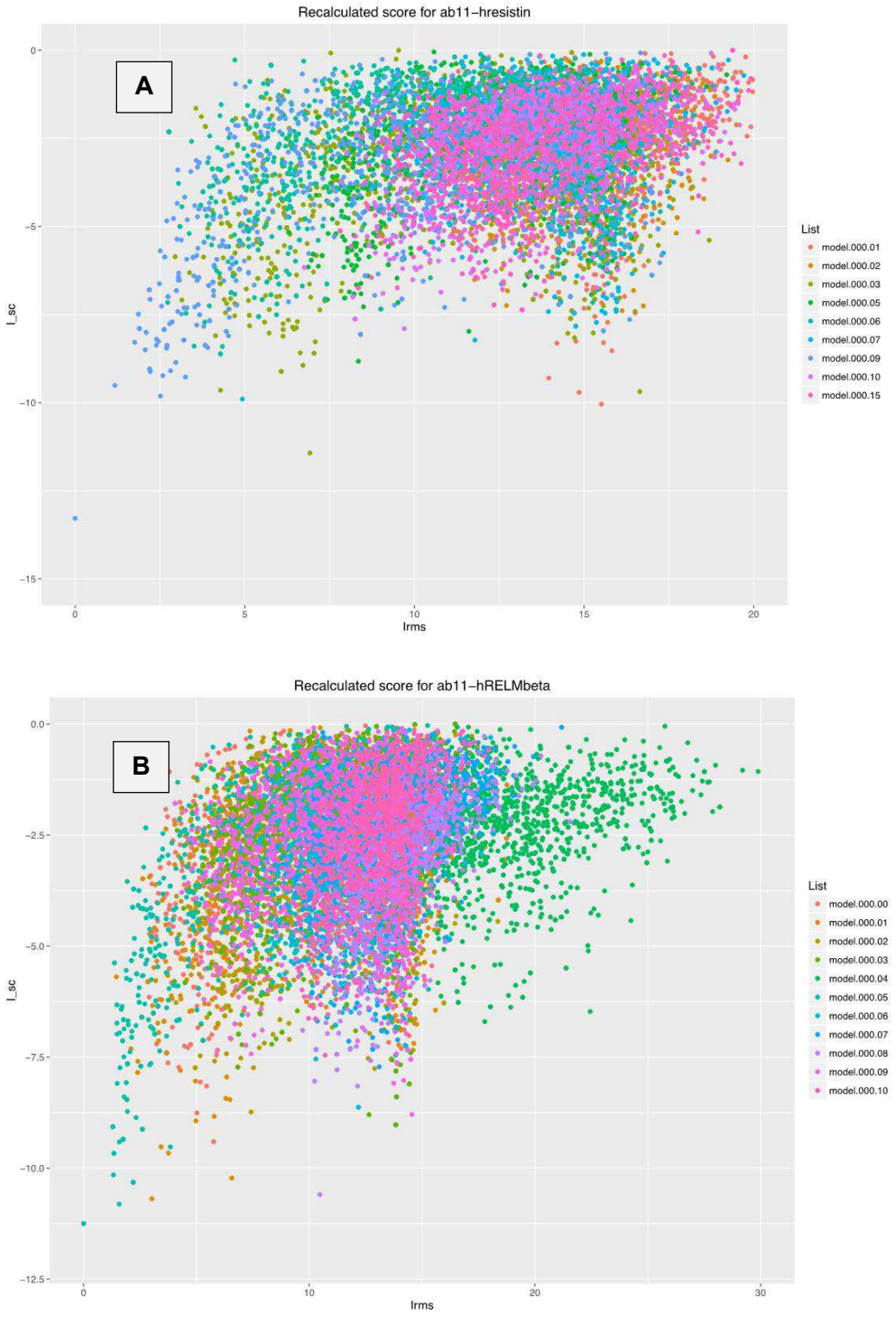

Figure.4.18: The docking results of AntiRes-11 with (A) hresistin and (B) hRELMβ showing strong convergence to the native structure suggesting true docked states.

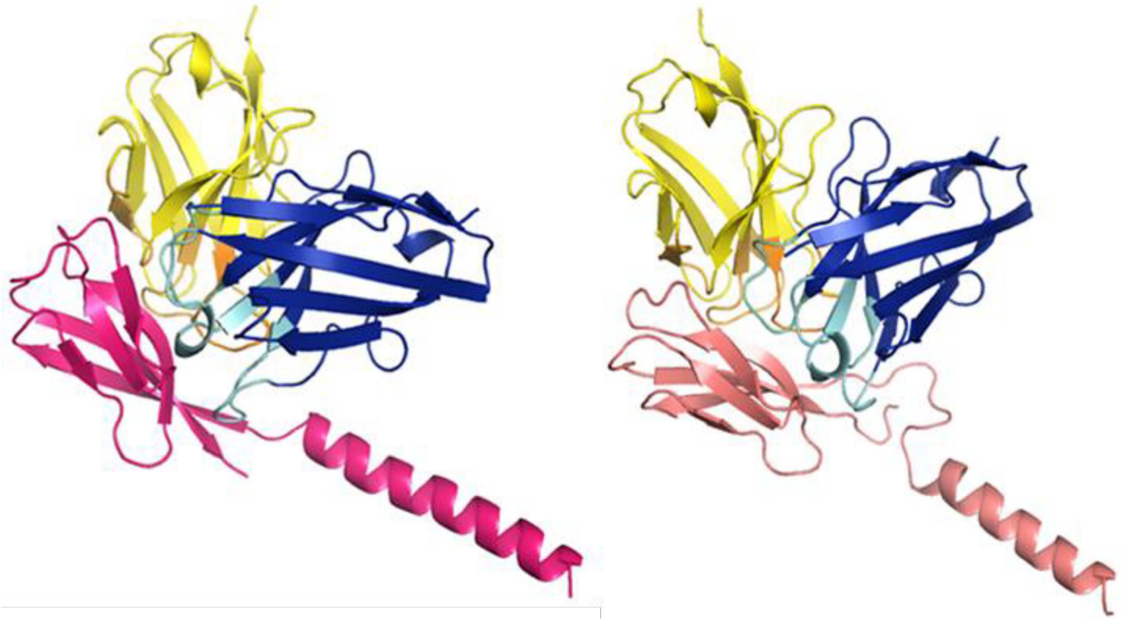

Figure.4.19: The final docked states of AntiRes-11 with hresistin (deep pink) and hRELMβ(salmon)

Overall, I could determine low energy structures of the antibodies docked to hresistin and hRELMβ. In some cases, I could predict confidently the binding regions while in other I wasn't able to computationally distinguish the most likley docked state from the false negatives especially in cases when the antibody tends to bind to the tail region (Table.4.1 and Table.4.2).

monomeric hresistin docked with antibodies		
Antibody	**Head**	**Tail**
AntiRes-2	**yes**	
AntiRes-3		yes

AntiRes-9	yes	
Antires-13	**yes**	
AntiRes-11	**yes**	

Table.4.1: Preferred docking positions of the antibodies to hresistin.

monomeric hRELMβ docked with antibodies		
Antibody	**Head**	**Tail**
AntiRes-2		yes
AntiRes-3		yes
AntiRes-9	**yes**	
AntiRes-13		yes
AntiRes-11	**yes**	

Table.4.2: Preferred docking positions of the antibodies to hRELMβ

Resistin Clone	Resistin Binding	RELMβ Binding	Resistin Blocking	RELMβ Blocking	Resistin Docking Lowest Energy Score(kcal /mol)	RELMβ Docking Lowest Energy Score(kcal/mol)
AntiRes-11	+	-	NA	NA	-13.29	-11.96
AntiRes-3	+	-	20-30%	30%	-11.23	-10.29
AntiRes-9	-	-	20%	10%	-10.58	-13.12
AntiRes-2	+	+	30-50%	30-50%	-28.67	-11.82
AntiRes-13	++	++++	100%	100%	-12.86	-11.57

Table.4.3:Comparison of lowest energy models docking scores with its experimental results.

Results from cell bioassay showed that antibodies AntiRes-13 and AntiRes-2 to both antigens and block its responses. From Table.4.1, Table.4.2 and Table.4.3 my docking results conclude that AntiRes-13 and AntiRes-2 docks to hresistin strongly but not so with hRELMβ as it prefers to dock to the tail region rather than head. As hresistin and hRELMβ have very strong homology in the head, I expect that the antibodies should bind to similar regions in both the antigens. To determine this, I compared the docking results of the antibodies with hresistin to the docking results with hRELMβ. This step helped me to determine if there is any consensus between the binding locations on hresistin and hRELMβ. This consensus would suggest that the models have captured the true binding site. Comparing the docking results, I determined that there isn't any consensus between the binding locations for both proteins (Figure.4.20). The results show that, I couldn't capture the true binding regions. This is because the initial starting position for docking in hresistin and hRELMβ are different. Both antibodies AntiRes-13 and AntiRes-2 showed similar outcome. This suggests that due to the hydrophobic residues present at the tail and the bent shape of the monomeric hRELMβ,

ClusPro and RosettaSnugDock couldn't capture the true binding site. To avoid this, a different approach will be required.

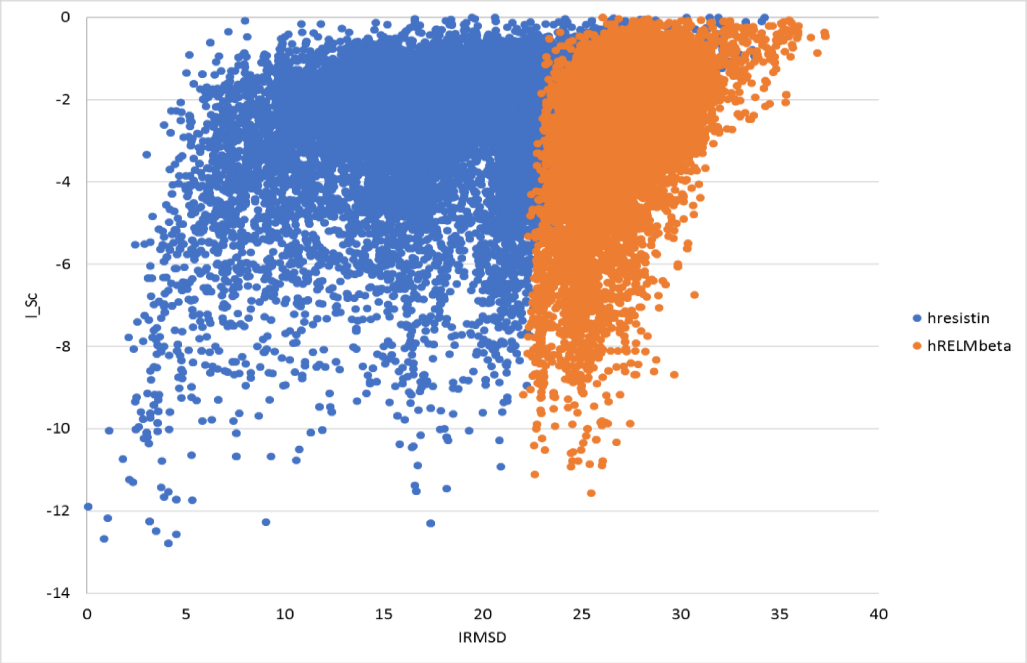

Figure.4.20: Comparison of the docking results of AntiRes-13 with hresistin (blue) to the docking results of AntiRes-13 with hRELM (orange). The results showed that there is no consensus in the binding locations.

CHAPTER V

CONCLUSION

I. Conclusion

In this project, I could predict preliminary structures of the monomer and hexamer (dimer of trimers) states of hresistin and hRELMβ. These modelled structures gave structural insight to the different states in nature. Also, I could successfully model all the 32 designed antibodies using RosettaAntibody. The modelled antibodies V_H-V_L orientations were within the natural structural parameters set by human antibodies. I could infer preliminary data of the different docked states of the various antibodies which experimentally bound to the hresistin and hRELMβ. In many of the cases I inferred converged results and could determine the epitope regions. But in some cases, there were discrepancies. This discrepancy in results could be caused due to preference of hydrophobic interactions by RosettaSnugDock or due to shape complementary by ClusPro. To avoid these discrepancy in the results, further analysis is required. This analysis could be performed by redocking the antibodies only to the head of the proteins, and compare the docking results. Removing the tail regions in the proteins will reduce the preference of hydrophobic interactions and give better docking results.

II. Future Work

Further work is required to successfully confirm my results. SAXS or crystallographic experiments can validate the predicted multimeric states of the proteins. The experiments will truly validate the different multimeric states and give better structural information of these proteins.

To avoid the discrepancies during antibody-antigen docking, we can refine our docking results by targeting only the head region of the proteins as they have strong homology, thus avoiding the tail which has strong hydrophobic residues. This will help to determine whether the antibodies preferring to bind at the tail, truly bind in that region or are false positive results. A quantitative assessment of the binding structure model quality is required to distinguish real and false-positive binders based on number and its comparison with experimental data. I need to check for consensus between the binding locations on hresistin and hRELMβ, as this consensus would suggest that the models capture the true binding site. To improve the binding affinities to the target regions, we can mutate the antibody sequences. Thus, designing better and improved antibodies from existing data. All these analyses will give a deeper insight in developing potential therapeutic models for curing PH.

References

1"Pulmonary Arterial Hypertension - NORD (National Organization for Rare Disorders)". NORD..

2. "Pulmonary arterial hypertension". Genetics Home Reference. January 2016. Retrieved 30 July 2017.

3. "Who Is at Risk for Pulmonary Hypertension? - NHLBI, NIH". NHLBI. 2 August 2011. Retrieved 30 July 2017.

4. "What Causes Pulmonary Hypertension? - NHLBI, NIH". NHLBI. 2 August 2011. Retrieved 30 July 2017.

5. "How Is Pulmonary Hypertension Treated? - NHLBI, NIH". NHLBI. 2 August 2011. Retrieved 30 July 2017.

6. "What Is Pulmonary Hypertension? - NHLBI, NIH". NHLBI. 2 August 2011. Retrieved 30 July 2017.

7. von Romberg, Ernst (1891–1892). "Über Sklerose der Lungenarterie". Dtsch Arch Klin Med (in German). 48: 197–206.

8. Diller, Gerhard-Paul; Gatzoulis, Michael A. (27 February 2007). "Pulmonary vascular disease in adults with congenital heart disease". Circulation. 115 (8): 1039–1050. ISSN 1524-4539. PMID 17325254. doi:10.1161/CIRCULATIONAHA.105.592386.

9. Angelini DJ, Su Q, Yamaji-Kegan K, Fan C, Skinner JT, Champion HC, Crow MT, Johns RA: Hypoxia-Induced Mitogenic Factor (HIMF/FIZZ1/RELM{alpha}) Induces the Vascular and Hemodynamic Changes of Pulmonary Hypertension. Am J Physiol Lung Cell Mol Physiol 2009.

10. Su Q, Zhou Y, Johns RA: Bruton's Tyrosine Kinase (BTK) is a Binding Partner for Hypoxia Induced Mitogenic Factor (HIMF/FIZZ1) and Mediates Myeloid Cell Chemotaxis. FASEB Journal 2008, In press.

11. Teng X, Li D, Champion HC, Johns RA: FIZZ1/RELMalpha, a novel hypoxia-induced mitogenic factor in lung with vasoconstrictive and angiogenic properties. Circ Res 2003, 92:1065-7.

12. Wagner KF, Hellberg AK, Balenger S, Depping R, Dodd OJ, Johns RA, Li D: Hypoxia-induced mitogenic factor has antiapoptotic action and is upregulated in the developing lung: coexpression with hypoxia-inducible factor-2alpha. Am J Respir Cell Mol Biol 2004, 31:276-82.

13. Yamaji-Kegan K, Su Q, Angelini DJ, Champion HC, Johns RA: Hypoxia-induced mitogenic factor has proangiogenic and proinflammatory effects in the lung via VEGF and VEGF receptor-2. Am J Physiol Lung Cell Mol Physiol 2006, 291:L1159-68.

14. Fan C, Meuchel LW, Su Q, Angelini DJ, Zhang A, Cheadle C, Kolosova I, Makarevich OD, Yamaji-Kegan K, Rothenberg ME, Johns RA: Resistin-Like Molecule alpha in Allergen-Induced Pulmonary Vascular Remodeling. Am J Respir Cell Mol Biol 2015, 53:303-13.

15. Angelini DJ, Su Q, Yamaji-Kegan K, Fan C, Teng X, Hassoun PM, Yang SC, Champion HC, Tuder RM, Johns RA: Resistin-like Molecule-{beta} (RELM{beta}) in Scleroderma-associated Pulmonary Hypertension. Am J Respir Cell Mol Biol 2009.

16. Chemaly ER, Hadri L, Zhang S, Kim M, Kohlbrenner E, Sheng J, Liang L, Chen J, P KR, Hajjar RJ, Lebeche D: Long-term in vivo resistin overexpression induces myocardial dysfunction and remodeling in rats. J Mol Cell Cardiol 2011, 51:144-55.

17. Kang S, Chemaly ER, Hajjar RJ, Lebeche D: Resistin promotes cardiac hypertrophy via the AMP-activated protein kinase/mammalian target of rapamycin (AMPK/mTOR) and c-Jun N-terminal kinase/insulin receptor substrate 1 (JNK/IRS1) pathways. The Journal of biological chemistry 2011, 286:18465-73.

18. Kim M, Oh JK, Sakata S, Liang I, Park W, Hajjar RJ, Lebeche D: Role of resistin in cardiac contractility and hypertrophy. J Mol Cell Cardiol 2008, 45:270-80.

19. Gerstmayer B, Kusters D, Gebel S, Muller T, Van Miert E, Hofmann K, Bosio A: Identification of RELMgamma, a novel resistin-like molecule with a distinct expression pattern. Genomics 2003, 81:588-95.

20. Holcomb IN, Kabakoff RC, Chan B, Baker TW, Gurney A, Henzel W, Nelson C, Lowman HB, Wright BD, Skelton NJ, Frantz GD, Tumas DB, Peale FV, Jr., Shelton DL, Hebert CC: FIZZ1, a novel cysteine-rich secreted protein associated with pulmonary inflammation, defines a new gene family. Embo J 2000, 19:4046-55.

21. Steppan CM, Brown EJ, Wright CM, Bhat S, Banerjee RR, Dai CY, Enders GH, Silberg DG, Wen X, Wu GD, Lazar MA: A family of tissue-specific resistin-like molecules. Proceedings of the National Academy of Sciences of the United States of America 2001, 98:502-6.

22. Yang RZ, Huang Q, Xu A, McLenithan JC, Eisen JA, Shuldiner AR, Alkan S, Gong DW: Comparative studies of resistin expression and phylogenomics in human and mouse. Biochem Biophys Res Commun 2003, 310:927-35.

23. Altschul, S.F., Gish, W., Miller, W., Myers, E.W. & Lipman, D.J. (1990) "Basic local alignment search tool." J. Mol. Biol. 215:403-410.

24. Gish, W. & States, D.J. (1993) "Identification of protein coding regions by database similarity search." Nature Genet. 3:266-272.

25. Madden, T.L., Tatusov, R.L. & Zhang, J. (1996) "Applications of network BLAST server" Meth. Enzymol. 266:131-141.

26. Altschul, S.F., Madden, T.L., Schäffer, A.A., Zhang, J., Zhang, Z., Miller, W. & Lipman, D.J. (1997) "Gapped BLAST and PSI-BLAST: a new generation of protein database search programs." Nucleic Acids Res. 25:3389-3402.

27. Zhang Z., Schwartz S., Wagner L., & Miller W. (2000), "A greedy algorithm for aligning DNA sequences" J Comput Biol 2000; 7(1-2):203-14.

28. Zhang, J. & Madden, T.L. (1997) "PowerBLAST: A new network BLAST application for interactive or automated sequence analysis and annotation." Genome Res. 7:649-656.

29. Morgulis A., Coulouris G., Raytselis Y., Madden T.L., Agarwala R., & Schäffer A.A. (2008) "Database indexing for production MegaBLAST searches." Bioinformatics 15:1757-1764.

30. Camacho C., Coulouris G., Avagyan V., Ma N., Papadopoulos J., Bealer K., & Madden T.L. (2008) "BLAST+: architecture and applications." BMC Bioinformatics 10:421.

31. Boratyn GM, Schäffer AA, Agarwala R, Altschul SF, Lipman DJ, & Madden T.L. (2012) "Domain enhanced lookup time accelerated BLAST." Biol Direct. 2012 Apr 17;7:12.

32. Biasini M, Bienert S, Waterhouse A, Arnold K, Studer G, Schmidt T, Kiefer F, Cassarino TG, Bertoni M, Bordoli L, Schwede T (2014). SWISS-MODEL: modelling protein tertiary and quaternary structure using evolutionary information Nucleic Acids Research 2014 (1 July 2014) 42 (W1): W252-W258

33. Kiefer F, Arnold K, Künzli M, Bordoli L, Schwede T (2009). The SWISS-MODEL Repository and associated resources. Nucleic Acids Res. 37, D387-D392.

34. Arnold K, Bordoli L, Kopp J, and Schwede T (2006). The SWISS-MODEL Workspace: A web-based environment for protein structure homology modelling. Bioinformatics.,22,195-201.

35. Guex, N., Peitsch, M.C. Schwede, T. (2009). Automated comparative protein structure modeling with SWISS-MODEL and Swiss-PdbViewer: A historical perspective. Electrophoresis, 30(S1), S162-S173.

36. B. Webb, A. Sali. Comparative Protein Structure Modeling Using Modeller. Current Protocols in Bioinformatics, John Wiley & Sons, Inc., 5.6.1-5.6.32, 2014.

37. M.A. Marti-Renom, A. Stuart, A. Fiser, R. Sánchez, F. Melo, A. Sali. Comparative protein structure modeling of genes and genomes. Annu. Rev. Biophys. Biomol. Struct. 29, 291-325, 2000.

38. A. Sali & T.L. Blundell. Comparative protein modelling by satisfaction of spatial restraints. J. Mol. Biol. 234, 779-815, 1993.

39. A. Fiser, R.K. Do, & A. Sali. Modeling of loops in protein structures, Protein Science 9. 1753-1773, 2000.

40. Sievers F, Wilm A, Dineen DG, Gibson TJ, Karplus K, Li W, Lopez R, McWilliam H, Remmert M, Söding J, Thompson JD, Higgins D, Molecular Systems Biology 7 Article number: 539 doi:10.1038/msb.2011.75

41. Goujon M, McWilliam H, Li W, Valentin F, Squizzato S, Paern J, Lopez R, Nucleic acids research 2010 Jul, 38 Suppl: W695-9 doi:10.1093/nar/gkq313

42. McWilliam H, Li W, Uludag M, Squizzato S, Park YM, Buso N, Cowley AP, Lopez R, Nucleic acids research 2013 Jul;(Web Server issue):W597-600 doi:10.1093/nar/gkt376

43. Nivón LG, Moretti R, Baker D (2013) A Pareto-Optimal Refinement Method for Protein Design Scaffolds. PLoS ONE 8(4): e59004. Paper

44. P. Conway, M. Tyka, F. DiMaio*, D. Konerding and D. Baker (2013). Relaxation of backbone bond geometry improves protein energy landscape modeling. Protein Science

45. Firas Khatib,Seth Cooper,Michael D. Tyka,Kefan Xu, Ilya Makedon,Zoran Popović,David Baker, and Foldit Players (2011)."Algorithm discovery by protein folding game players", PNAS 2011 108 (47) 18949-18953;

46. Tyka MD, Keedy DA, Andre I, Dimaio F, Song Y, et al. (2011) "Alternate states of proteins revealed by detailed energy landscape mapping". Journal of molecular biology 405: 607–618.

47. B. D. Weitzner, J. R. Jeliazkov, S. Lyskov, N. M. Marze, D. Kuroda, R. Frick, J. Adolf-Bryfogle, N. Biswas, R. L. Dunbrack Jr., and J. J. Gray, "Modeling and docking of antibody structures with Rosetta." Nature Protocols 12, 401–416 (2017)

48. B. D. Weitzner, D. Kuroda, N. M. Marze, J. Xu & J. J. Gray, "Blind prediction performance of RosettaAntibody 3.0: Grafting, relaxation, kinematic loop modeling, and full CDR optimization." Proteins 82(8), 1611–1623 (2014)

49. A. Sivasubramanian, A. Sircar, S. Chaudhury & J. J. Gray, "Toward high-resolution homology modeling of antibody Fv regions and application to antibody-antigen docking," Proteins 74(2), 497–514 (2009)

50. J. Xu, D. Kuroda & J. J. Gray, “RosettaAntibody3: Object-Oriented Designed Protocol and Improved Antibody Homology Modeling.” (2013)

51. Chothia C, Lesk AM. Canonical structures for the hypervariable regions of immunoglobulins. J. Mol. Biol. 1987; 196:901-17.

52. Al-Lazikani B, Lesk AM, Chothia C. Standard conformations for the canonical structures of immunoglobulins. J. Mol. Biol. 1997;273:927-48.

53. North, B, Lehmann A, Dunbrack R. A new clustering of antibody CDR loop conformations: J. Mol. Biol. (2011), 406(2): 228-256.

54. Kozakov D, Hall DR, Xia B, Porter KA, Padhorny D, Yueh C, Beglov D, Vajda S. The ClusPro web server for protein-protein docking. Nature Protocols. 2017 Feb;12(2):255-278

55. Kozakov D, Beglov D, Bohnuud T, Mottarella S, Xia B, Hall DR, Vajda, S. How good is automated protein docking? Proteins: Structure, Function, and Bioinformatics, 2013 Aug

56. Kozakov D, Brenke R, Comeau SR, Vajda S. PIPER: An FFT-based protein docking program with pairwise potentials. Proteins. 2006 Aug 24

57. Comeau SR, Gatchell DW, Vajda S, Camacho CJ. ClusPro: an automated docking and discrimination method for the prediction of protein complexes. Bioinformatics. 2004 Jan 1

58. Comeau SR, Gatchell DW, Vajda S, Camacho CJ. ClusPro: a fully automated algorithm for protein-protein docking Nucleic Acids Research. 2004 Jul 1

59. Brenke R, Hall DR, Chuang G-Y, Comeau SR, Bohnuud T, Beglov D, Schueler-Furman O, Vajda S, Kozakov D. 2012. Application of asymmetric statistical potentials to antibody-protein docking. Bioinformatics. 28(20):2608-2614

60. A. Sircar & J. J. Gray "SnugDock: Paratope structural optimization during antibody-antigen docking compensates for errors in antibody homology models," PLoS Comput. Biol. 6(1) (2010)

61. Patel SD, Rajala MW, Rossetti L, Scherer PE, Shapiro L." Disulfide-dependent multimeric assembly of resistin family hormones",Science. 2004 May 21;304(5674):1154-8

62. Shaudhury, M. Berrondo, B. D. Weitzner, P. Muthu, H. Bergman, & J. J. Gray "Benchmarking and analysis of protein docking performance in RosettaDock 3.2," PLoS One 6(8) (2011)

Curriculum Vitae

1. **Name** : NAIREETA BISWAS
2. **Gender** : Female
3. **Date of Birth** : 9th February 1993
4. **Permanent Address** : Qr. No. A0, Director's Residence
   National Institute of Technology Rourkela,
   Rourkela – 769008, Odisha, India
5. **Email id.** : **naireeta1993@gmail.com**
6. **Phone Number** : +91 9035171060

7. **Academic Qualifications:**

DEGREE	*INSTITUTE/UNIVERSITY*	*YEAR OF COMPLETION*	*PRECENTAGE/ GRADE*	*SPECIALIZATION*
Class X Matriculation	Delhi Public School, Kalyanpur, India (CBSE Board)	2008	90.04%	Science
Class XII High School	Delhi Public School, Kalyanpur, India (CBSE Board)	2010	76.8%	Physics, Chemistry,Mathematics,Biotechnology
B.Tech	Manipal Institute of Technology, Manipal, India	2015	8.46/10	Chemical Engineering
M.S.E	Johns Hopkins University, Baltimore,U.S.A	2017	3.36/4	Chemical and Biomolecular Engineering

8. Awards:

• Awarded the **ChemBE Master's Essay Scholarship** by the Department of Chemical and Biomolecular Engineering at Johns Hopkins University for the fall 2016 and spring 2017 semesters. • Recipient of "**Certificate of Merit"** in All India Talent Search Examination (ClassXI) conducted by "**Children's education Trust**".

9. Research:

- **Master's Thesis:** Structural modelling of the Resistin and RELM family proteins and its cognate antibodies for developing potential therapeutics against Pulmonary Hypertension

  Advisor: Prof. Jeffrey J. Gray (jgray@jhu.edu)

  Collaboration: Prof. Roger Johns, Johns Hopkins School of Medicine (rajohns@jhmi.edu)

Other work during master's degree: Structural comparison of set of naïve and antigen exposed public antibodies to determine inherent properties.

Advisor: Prof. Jeffrey J. Gray (jgray@jhu.edu)

Undergraduate: Shuheng (Kathy) Wang, ChemBE Junior, JHU

- **B.Tech Thesis:** Rheological behavior of Garamite Clay Dispersion

  Advisor: Prof. Yogesh M. Joshi(joshi@iitk.ac.in)

10. Summer Research Internships:

a. **Title of the project** : Characterization of functionalized Multi walled Carbon Nanotubes and preparation of epoxy – CNT nanocomposites.

Duration : 1st June, 2012 to 29th July, 2012

Institute : Indian Institute of Space Science and Technology, Trivandrum, Kerala **Name of Supervisor** : Dr. N. Gomathi (gomathi@iist.ac.in)

Equipment Used : FTIR spectroscopy, SEM, DSC, TGA

b. **Title of the project** : Cloning, purification and crystallization of the protein Tear GD1 from *Thermotoga maritima* to determine its 3D structure using X- ray diffraction technique.

Duration : 1st June, 2013 to 6th August, 2013

Institute : Indian Institute of Technology Kanpur, Kanpur, U.P

Name of Supervisor : Prof. Balaji Prakash (bprakash@iitk.ac.in)

Equipment Used : AKTA (for purification purpose), PCR Thermocycle setup, Mosquito (for crystallization)

c. **Title of the project**: Characterization and synthesis of Graphene using Chemical Vapor Deposition method.

Duration : 20st June, 2013 to 6th August, 2013

Institute : Indian Institute of Technology Kanpur, Kanpur, U.P

Name of Supervisor : Prof. Kamal K. Kar (kamalkk@iitk.ac.in)

Equipment Used : Raman spectroscopy, AFM (atomic forced microscopy), DSC, TGA

d. **Title of the project**: Rheology analysis of Polyacrylamide

Duration : 16th December 2013 to 13th January 2014

Institute : Indian Institute of Technology Kanpur, Kanpur, U.P **Name of Supervisor** :Prof. Yogesh M. Joshi(joshi@iitk.ac.in)

Equipment Used : Rheometer

e. **Title of the project**: Predicting the growth behavior in a novel biochemical pathway model

Duration : 28th May 2014 to 1st August 2014

Institute : Technische Universität München, München, Germany

Name of Supervisor : Prof. Dr.-Ing. Habil. Andreas Kremling(a.kremling@lrz.tumuenchen.de)

14. Paper Published/Accepted:

- Weitzner BD, Jeliazkov JR, Lyskov S, Marze N, Kuroda D, Frick R, Adolf-Bryfogle A, **Biswas N** & Gray JJ "**Modeling and docking antibody structures with Rosetta**," *Nature Protocols* **12**, 401–416 (2017)

- N. Gomathi, L. G. Nair, J. Lavanya**, N. Biswas**, K. Joseph, C. P. Reghunadhan Nair, S. Neogi, "**RF plasma method - a straightforward, dry means for functionalization of carbon nanotubes**", accepted for presentation in **International Symposium on Plasma Chemistry,** Cairns, Australia, 4-9th August, 2013

Currently in the process of writing a paper based on my Master's thesis work. This paper will include my work on **structural modeling of Resistin proteins with its cognate antibodies to develop potential therapeutics for Pulmonary Hypertension.**

15. Review Paper Presented:

- **Naireeta Biswas**, D. Neha Reddy, "**Milking of diatoms for the generation of biodiesel**" in the event Chemignite organized by **Indian Institute of Chemical Engineers** (IIChE) Student Chapter Manipal, Manipal University, September, 2012.

16. Poster Presentation:

- Presented a poster on " **Structural modelling of Resistin and RELM family proteins and their cognate antibodies**" at the ChemBE recruitment weekend held on March 18th , 2016

17. Conferences Attended:

- Attended the **Winter's RosettaCon** held at San Diego, California from February 7th to February 10th 2017

- Attended the **Grace Hopper Celebration for Women in Computing** held at Houston, Texas from October 18th to October 22nd, 2016

- Attended the annual **IBR Retreat** organized by the Bio-Physics Department of Johns Hopkins University.

18. Teaching Experience:

- Teaching Assistant for the undergraduate course Chemical Engineering Lab for the fall 2015

- Part of the STEM Achievement in Baltimore Elementary Schools (SABES) program mentoring 4th grade students once a week

- Mentoring undergraduate student Shuheng (Kathy) Wang, a member of the Gray Lab

19. Extra-Curricular Activity:

- Member of the **Rosetta Commons** as a developer
- Member of the Working committee of **IIChE, Student Chapter of Manipal Branch.**
- Member of the organizing committee of **CHEMOTHON** organized by **IIChE, India** as the part of Technical festival at MIT, Manipal.
- North zone **champion** in inter-CBSE school meet in **swimming** in 2005,2004
- Participated **national** level CBSE board **swimming championship** in 2005.
- Passed with **distinction** up to 3rd year in **Violin** from Akhil Bharatiya Gandharv Mahavidyalaya.
- Enjoy **painting and sketching** and received **prizes** in local **competition**.
- Member of the organizing committee of "**PANORAMA** "a cultural festival organized by Delhi Public School, Kalyanpur, Kanpur.